

1 **The revised parts are highlighted by blue**

2 **Title:** Decadal variation of CO₂ fluxes and its budget in a wheat and maize rotation cropland
3 over the North China Plain

4 Quan Zhang^{1,2}, Huimin Lei², Dawen Yang², Lihua Xiong¹, Pan Liu¹, Beijing Fang^{2,3}

5 ¹State Key Laboratory of Water Resources and Hydropower Engineering Science, Wuhan

6 University, Wuhan, China

7 ²State Key Laboratory of Hydrosience and Engineering, Department of Hydraulic

8 Engineering, Tsinghua University, Beijing, China

9 ³Department of Civil and Environmental Engineering, The Hong Kong University of Science

10 and Technology, Hong Kong SAR, China

11 Correspondence to:

12 Q. Zhang (quan.zhang@whu.edu.cn) and H. Lei (leihm@tsinghua.edu.cn)

13 Tel: 86-(0)10-6278-3383

14 Fax: 86-(0)10-6279-6971

15 **This work is distributed under the Creative Commons Attribution 4.0 License**



17 **Abstract:**

18 Carbon sequestration in agro-ecosystems has great potentials to mitigate global greenhouse
19 gas emissions. To assess the decadal trend of CO₂ fluxes of an irrigated wheat-maize rotation
20 cropland over the North China Plain, the net ecosystem exchange (NEE) with the atmosphere
21 was measured by using an eddy covariance system from 2005 through 2016. To evaluate the
22 detailed CO₂ budget components of this representative cropland, a comprehensive experiment
23 was conducted in the full 2010-2011 wheat-maize rotation cycle by combining the eddy
24 covariance NEE measurements, plant carbon storage samples, a soil respiration experiment
25 that differentiated between heterotrophic and below-ground autotrophic respirations. Over the
26 past decade from 2005 through 2016, the cropland exhibited a decreasing carbon
27 sequestration capacity; the average of total NEE, Gross Primary Productivity (GPP),
28 Ecosystem Respiration (ER) for wheat were -364, 1174 and 810 gC m⁻², and were -136,
29 1008, and 872 gC m⁻² for maize. The multiple regression revealed that, air temperature and
30 groundwater depth showed pronounced correlation with the CO₂ fluxes for wheat; but in the
31 maize season, incoming short-wave radiation and groundwater depth showed pronounced
32 correlations with CO₂ fluxes. For the full 2010-2011 agricultural cycle, the CO₂ fluxes for
33 wheat and maize were as follows: NEE -438 and -239 gC m⁻², GPP 1078 and 780 gC m⁻², ER
34 640 and 541 gC m⁻², soil heterotrophic respiration 377 and 292 gC m⁻², below-ground
35 autotrophic respiration 136 and 115 gC m⁻², above-ground autotrophic respiration 128 and
36 133 gC m⁻²; the net biome productivity was 59 gC m⁻² for wheat and 5 gC m⁻² for maize,
37 indicating that wheat was a weak CO₂ sink and maize was close to CO₂ neutral to the
38 atmosphere for this agricultural cycle. However, when considering the total CO₂ loss in the

39 fallow period, the net biome productivity was $-40 \text{ gC m}^{-2} \text{ yr}^{-1}$ for the full 2010-2011 cycle,
40 implying that the cropland was a weak CO₂ source. The investigations of this study showed
41 that taking cropland as a climate change mitigation tool is challenging and further studies are
42 required for the CO₂ sequestration potential of croplands.

43 **Key words:** Cropland; CO₂; Decadal trend; Maize; North China Plain; Wheat

44 **Introduction**

45 The widely used eddy covariance technique (Aubinet et al., 2000; Baldocchi et al., 2001;
46 Falge et al., 2002b) has enabled us to better understand the terrestrial CO₂ exchange with the
47 atmosphere, thereby forested our understanding of the mechanisms on how the terrestrial
48 ecosystems contribute to mitigate the ongoing climate change (Falkowski et al., 2000; Gray et
49 al., 2014; Poulter et al., 2014; Forkel et al., 2016). Agro-ecosystems play an important role in
50 regulating the global carbon balance (Lal, 2001; Bondeau et al., 2007; Özdoğan, 2011; Taylor
51 et al., 2013; Gray et al., 2014) and are believed to have great potentials to mitigate global
52 carbon emissions through cropland management (Sauerbeck, 2001; Freibauer et al., 2004;
53 Smith, 2004; Hutchinson et al., 2007; van Wesemael et al., 2010; Ciais et al., 2011; Schmidt et
54 al., 2012), furthermore, some studies proposed the agro-ecosystems as the “natural climate
55 solutions” to mitigate global carbon emission (e.g., Griscom et al., 2017; Fargione et al.,
56 2018). The field management practices (e.g., irrigation, fertilization and residue removal, etc.)
57 impact the cropland CO₂ fluxes (Baker and Griffis, 2005; Béziat et al., 2009; Ceschia et al.,
58 2010; Eugster et al., 2010; Drewniak et al., 2015; de la Motte et al., 2016; Hunt et al., 2016;
59 Vick et al., 2016), but their relative importance in determining the cropland CO₂ budget
60 remain unclear because of limited field observations (Kutsch et al., 2010), motivating
61 comprehensive CO₂ budget assessments across different cropland management styles.

62 Over the past two decades, CO₂ investigations of agro-ecosystems have mainly focused on the
63 variations in the net ecosystem exchange with the atmosphere (i.e., NEE) or its two derived
64 components (i.e., GPP and ER) using the eddy covariance. To date, these evaluations have

65 been widely conducted for wheat (Gilmanov et al., 2003; Anthoni et al., 2004a; Moureaux et
66 al., 2008; Béziat et al., 2009; Vick et al., 2016), maize (Verma et al., 2005), sugar beet
67 (Aubinet et al., 2000; Moureaux et al., 2006), potato (Anthoni et al., 2004b; Fleisher et al.,
68 2008), soybean-maize rotation cropland (Gilmanov et al., 2003; Hollinger et al., 2005; Suyker
69 et al., 2005; Verma et al., 2005; Grant et al., 2007), and winter wheat-summer maize cropland
70 (Zhang et al., 2008; Lei and Yang, 2010). However, the long-term variations of the cropland
71 CO₂ fluxes remain limited, leaving our knowledge of the cropland potential as the future
72 climate change mitigation tool incomplete.

73 The widely used eddy covariance technique has fostered our understanding of the integrated
74 fluxes of NEE, GPP and ER, but cannot provide the detailed CO₂ budget components, which
75 consist of carbon assimilation (i.e., GPP), soil heterotrophic respiration (R_H), above-ground
76 autotrophic respiration (R_{AA}), below-ground autotrophic respiration (R_{AB}), lateral carbon
77 export at harvest and import at sowing or through organic fertilization (Ceschia et al., 2010).
78 These different CO₂ components result from different biological and biophysical processes
79 (Moureaux et al., 2008) that may respond differently to climatic conditions, environmental
80 factors and management strategies (Ekblad et al., 2005; Zhang et al., 2013). Differentiating
81 among these components is a prerequisite for understanding the response of terrestrial
82 ecosystems to changing environment (Heimann and Reichstein, 2008), so the carbon budget
83 evaluations have been reported for a few croplands (e.g., Moureaux et al., 2008; Ceschia et
84 al., 2010; Wang et al., 2015; Demyan et al., 2016; Gao et al., 2017). In particular, to account
85 for the literal carbon export, the Net Biome Productivity (NBP) is often estimated by

86 combining the eddy covariance technique and field carbon measurements associated with
87 harvests and residue treatments (Ceschia et al., 2010; Kutsch et al., 2010). As detailed CO₂
88 budget might facilitate better predictions of agro-ecosystems' responses to climate change, the
89 CO₂ budget evaluations in different croplands remain necessary.

90 The North China Plain (NCP) is one of the most important food production regions in China,
91 and it guarantees the national food security by providing more than 50% and 33% of the nation's
92 wheat and maize, respectively (Kendy et al., 2003). Irrigation by diverting water from the
93 Yellow River is common to alleviate the water stress during spring in the NCP, resulting in a
94 very shallow groundwater depth (usually range from 2 to 4 m) along the Yellow River (Cao et
95 al., 2016) (Fig. 1). Wang et al. (2015) suggested that a groundwater-fed cropland in the NCP
96 had been losing carbon, and other studies also reported croplands in this region as carbon
97 sources (e.g., Li et al., 2006; Luo et al., 2008). However, the long-term variations (e.g., >10
98 years) of the CO₂ fluxes over the NCP remain lacking, leaving the trend of carbon sequestration
99 capacity of this region unknown.

100 To this end, this study is designed to assess the long-term variation of CO₂ fluxes and its
101 budget of the representative wheat-maize rotation cropland in the NCP. The eddy covariance
102 system was used to measure the CO₂ exchange from 2005 through 2016. For the full 2010-
103 2011 agricultural cycle, we measured soil respiration and sampled crops to quantify the
104 detailed CO₂ budget components. These measurements allow to (1) investigate the decadal
105 CO₂ flux (NEE, GPP, and ER) trend over this cropland; (2) provide the detailed CO₂ budget
106 components; and (3) estimate the Net Primary Productivity (NPP), Net Ecosystem

107 Productivity (NEP), and Net Biome Productivity (NBP).

108 **Materials and methods**

109 **Site description and field management**

110 The experiment was conducted in a rectangular-shaped (460 m × 280 m) field of the
111 representative cropland over the NCP (36° 39' N, 116° 03' E, Weishan site of Tsinghua
112 University, Fig. 1). The soil is silt loam with the field capacity of 0.33 m³ m⁻³ and saturation
113 point of 0.45 m³ m⁻³ for the top 5 cm soil. The mean annual precipitation is 532 mm and the
114 mean air temperature is +13.3 °C. The winter wheat-summer maize rotation system is the
115 representative cropping style in this region. On average, the winter wheat is sown around
116 October 17th and harvested around June 16th of the following year with crop residues left on
117 the field; summer maize is sown following the wheat harvest around June 17th and harvested
118 around October 16th. Prior to sowing wheat of the next season, the field is thoroughly
119 ploughed to fully incorporate maize residues into the top 20 cm soil. The canopies of both
120 wheat and maize are very uniform across the whole season. Nitrogen fertilizer is commonly
121 applied at this site with the amount of 35 gN m⁻² for wheat and 20 gN m⁻² for maize. The crop
122 density is 775 plants m⁻² for wheat with a ridge spacing of 0.26 m, and 4.9 plants m⁻² for
123 maize with a ridge spacing of 0.63 m, on average. Wheat is commonly irrigated with water
124 diverted from the Yellow River and the irrigation is about 150 mm every year; maize is rarely
125 irrigated because of the high precipitation in the summer. [During the 2010-2011 agricultural](#)
126 [cycle with CO₂ budget components evaluated, winter wheat was sown on October 23rd, 2010](#)
127 [and subsequently harvested on June 10th, 2011; summer maize was sown on June 23rd, 2011](#)

128 and harvested on September 30th, 2011. The entire year from October 23rd, 2010 through
129 October 22nd, 2011 was studied for the annual CO₂ budget evaluation.

130 (Fig. 1 here)

131 **Eddy covariance measurements**

132 A flux tower was set up at the center of the experiment field in 2005 (Lei and Yang, 2010;
133 Zhang et al., 2013). The NEE was measured at 3.7m above ground with an eddy covariance
134 system consisting of an infrared gas analyzer (LI-7500, LI-COR Inc., Lincoln, NE, USA) and
135 a three-dimensional sonic anemometer (CSAT3, Campbell Scientific Inc., Logan, UT, USA).
136 The 30-min averaged NEE was calculated from the 10 Hz raw measurements with TK2
137 (Mauder and Foken, 2004) from 2005 through 2012 and TK3 software package (Mauder and
138 Foken, 2011) from 2013 through 2016. The storage flux was calculated by assuming a
139 constant CO₂ concentration profile. Nighttime measurements under stable atmospheric
140 conditions with a friction velocity lower than 0.1 m s⁻¹ were removed from the analysis (Lei
141 and Yang, 2010). In the gap filling procedure, gaps less than 2 h were filled using linear
142 regression, while other short gaps were filled using the Mean Diurnal Variation (MDV)
143 method (Falge et al., 2001); gaps longer than 4 weeks were not filled. NEE was further
144 partitioned to derive GPP and ER using the nighttime method (Reichstein et al., 2005; Lei and
145 Yang, 2010), which assumes that daytime and nighttime ER follow the same temperature
146 response, thereby estimates the daytime ER using the regression model derived from the
147 nighttime measurements. In particular, this study adopted the method proposed by Reichstein
148 (2005) to quantify the short-term temperature sensitivity of ER from nighttime measurements

149 as described by the Vant Hoff equation,

$$150 \quad ER = ER_{\text{ref}} \exp(bT_s), \quad (1)$$

151 Where T_s is soil temperature, ER_{ref} is the reference respiration at 0 °C, and b is a parameter
152 associated with the commonly used temperature sensitivity coefficient Q_{10} ,

$$153 \quad Q_{10} = \exp(10b). \quad (2)$$

154 The long-term temperature sensitivity b of the season (either wheat or maize) was determined
155 by averaging all the estimated short-term b in each of the four-day window with the inverse of
156 the standard error as a weighing factor. The long-term temperature sensitivity b was then used
157 to estimate the ER_{ref} parameter in each of the four-day window by fitting the eq. (1), then
158 ER_{ref} of each day was estimated by using the least square spline approximation (Lei and Yang,
159 2010).

160 To quantify the contribution of source areas to the CO₂ flux measurement of the eddy
161 covariance, we used an analytical footprint model (Hsieh et al., 2000),

$$162 \quad f(\chi, z_m) = \frac{1}{\kappa^2 \chi^2} D z_u^P |L|^{1-P} \exp\left(\frac{-1}{\kappa^2 \chi} D z_u^P |L|^{1-P}\right) \quad (3)$$

163 where $D=0.28$ and $P=0.59$ are similarity constants for unstable condition (Hsieh et al., 2000),
164 $\kappa=0.4$ is von Karman constant, χ represents the horizontal coordinate, L represents the
165 Obukhov length, z_m represents the measurement height, and z_u represents the length scale
166 expressed as,

$$167 \quad z_u = z_m \left[\ln\left(\frac{z_m}{z_0}\right) - 1 + \frac{z_m}{z_0} \right] \quad (4)$$

168 where z_0 represents the zero displacement height.

169 Note that the eddy covariance system failed from October 23, 2010 to April 1, 2011 during the
170 wheat dormant season. To evaluate the seasonal CO₂ budget of this rotation cycle, the flux
171 gap of this period was filled by using the machine learning Support Vector Regression (SVR)
172 algorithm (Cristianini and Shave-Taylor, 2000), which has been proved to be an appropriate
173 tool for flux gap fillings (e.g., Kang et al., 2019; Kim et al., 2019) (see Appendix A).

174 **Meteorological and environmental condition measurements**

175 The meteorological variables were measured at 30-min intervals by a standard meteorological
176 station on the tower. Among these variables were the air temperature (T_a) and relative
177 humidity (RH) (HMP45C, Vaisala Inc, Helsinki, Finland) at the height of 1.6 m, precipitation
178 (P) (TE525MM, Campbell Scientific Inc), incoming short-wave radiation (R_{si}) (CRN1, Kipp
179 & Zonen, Delft, Netherlands) and photosynthetic photon flux density (PPFD) (LI-190SA, LI-
180 COR Inc) at the height of 3.7 m. The 30-min interval edaphic measurements included soil
181 temperature (T_s) (109-L, Campbell Scientific Inc.), volumetric soil moisture (θ) (CS616-L,
182 Campbell Scientific Inc.) for the top 5 cm soil; soil matric potential (ψ) (257-L, Campbell
183 Scientific Inc.) was measured since 2010 at the same depth. The groundwater depth (WD)
184 (CS420-L, Campbell Scientific Inc.) was measured at a location close to the meteorological
185 station in 30-min intervals.

186 **Biometric measurements and crop samples**

187 To trace crop development and carbon storage, we measured canopy height (H_C), plant area
188 index (PAI), crop dry matter (DM), and carbon content of crop organs at an interval of 7-10
189 days in the footprint of eddy covariance. Due to inclement weather, measurement intervals

190 were occasionally extended to two weeks or longer. The H_C was measured with a ruler and
191 PAI was measured with LAI-2000 (LI-COR Inc.) at ten locations randomly distributed in the
192 field. For crop samples, four locations were randomly selected at the start of the growing
193 season, crop samples were then collected close to these four locations throughout the
194 experimental period. At each location, 10 crop samples were collected for wheat and 3 crop
195 samples were collected from maize. To reduce the sample uncertainty at harvest, 200 crops
196 and 5 crops were collected in each location for wheat and maize, respectively. The crop
197 organs were separated and oven-dried at 105 °C for kill-enzyme torrefaction for 30 min, and
198 then oven-dried at 75 °C until a constant weight. The crop samples were used to estimate the
199 average field biomass (Dry Matter). The carbon content was analyzed using the combustion
200 oxidation-titration method (National Standards of Environmental Protection of the People's
201 Republic of China, 2013) to estimate carbon storage. The crop samples provided a direct
202 estimate of the Net Primary Productivity (NPP).

203 **Soil respiration measurements**

204 Soil respiration was measured every day in the footprint of the eddy covariance between
205 13:00 and 15:00 from March through September of 2011 using a portable soil respiration
206 system LI-8100 (LI-COR Inc.). Below-ground autotrophic respiration and heterotrophic
207 respiration were differentiated using the root exclusion method (Zhang et al., 2013). The total
208 soil respiration (R_S) and R_H were measured at treatments with and without roots, respectively,
209 and the corresponding difference is R_{AB} . To reduce the uncertainty associated with spatial
210 variability, we set three replicate pairs of comparative treatments (i.e., with root and without

211 root) randomly in the field. The uniform field condition contributes to reduce the
212 measurement uncertainty associated with the spatial variability (see Zhang et al., 2013). To
213 assess the seasonal variations and total amount of soil respirations, the seasonal continuous
214 R_H was constructed using the Q_{10} model by incorporating soil moisture as follows (Zhang et
215 al., 2013):

$$216 \quad R_H = A \exp(BT_s) \cdot f(\theta), \quad (4)$$

$$217 \quad f(\theta) = \begin{cases} 1, & \theta \leq \theta_f \\ a(\theta - \theta_f)^2 + 1, & \theta > \theta_f \end{cases}, \quad (5)$$

218 where θ_f is the field capacity. The parameters were inferred by fitting the R_H and T_s
219 measurements by using the least square method (see Zhang et al., 2013), where $A=1.16$,
220 $B=0.0503$, and $a=-44.9$ (see Zhang et al., 2013).

221 The R_{AB} of wheat was assumed to be 0 before March 14th due to the negligible plant biomass;
222 R_{AB} of other periods was estimated based on the R_H measurement and the ratio of the R_{AB} to
223 R_S estimated previously (Zhang et al., 2013), and the continuous R_{AB}/R_S ratio was
224 interpolated from the daily records (Fig. 2). This estimation method is robust because the
225 R_{AB}/R_S ratio is nearly constant around its diurnal average (Zhang et al., 2015b).

226 **(Fig. 2 here)**

227 **Synthesis of the CO₂ budget components**

228 The CO₂ budget components were derived by combining the eddy covariance measurements,
229 soil respiration experiments and crop samples. Eddy covariance-measured NEE is the
230 difference between carbon assimilation (i.e., GPP) and carbon release (i.e., ER). The ER

231 consists of R_H , R_{AB} (i.e., root respiration) and above-ground autotrophic respiration (R_{AA}).

232 The total soil respiration is the sum of R_H and R_{AB} ,

$$233 \quad R_S = R_H + R_{AB}. \quad (6)$$

234 The total autotrophic respiration (R_A) is the difference between the eddy covariance-derived
235 ER and R_H ,

$$236 \quad R_A = ER - R_H. \quad (7)$$

237 The above-ground autotrophic respiration (R_{AA}) is the difference between the eddy
238 covariance-derived ER and R_S in eq. (6),

$$239 \quad R_{AA} = ER - R_S. \quad (8)$$

240 NPP is plant biomass carbon storage, and can be quantified as the difference between GPP
241 and R_A ,

$$242 \quad NPP_{EC} = GPP - R_A, \quad (9)$$

243 where the subscript “EC” represents that the NPP is estimated from the eddy covariance-
244 derived GPP. In parallel, NPP can also be directly inferred from biomass samples as,

$$245 \quad NPP_{CS} = C_{cro}, \quad (10)$$

246 where the subscript “CS” indicates that NPP is based on crop samples, and C_{cro} is the plant
247 biomass carbon storage at harvest. [We used the average of the two independent NPPs as the](#)
248 [measurement for this site.](#)

249 NEP is commonly estimated by the NEE measurement ($NEP_{EC} = -NEE$). In this study, the crop
250 samples and soil respiration measurements also provided an independent estimate as,

251 $NEP_{CS}=NPP_{CS}-R_H$. (11)

252 We used the average of the two NEPs as the measurement for this site.

253 At this site, there were no fire and insect disturbances, and there was no manure fertilizer
254 application. The carbon input from seeds was negligible, and all crop residues were returned
255 to the field. Thus, NBP can be quantified as the difference between NEP and grain export
256 carbon loss (C_{gra}),

257 $NBP=NEP-C_{gra}$, (12)

258 **Results**

259 **Meteorological conditions and crop development**

260 The inter-annual variations of major meteorological variables are shown in Fig. 3, and they
261 showed no clear trend for both wheat and maize seasons. For the full 2010-2011 cycle with
262 comprehensive experiments, the average R_{si} and T_a were very close to other years; however,
263 the P during maize season was a little higher than other years (Fig. 3c), leading to a shallow
264 WD in maize season (Fig. 3d). The intra-annual variations of field microclimates for the full
265 2010-2011 cycle are shown in Fig. 4. The seasonal maximum and minimum T_a occurred in
266 July and January, respectively, and the variations in vapor pressure deficit (VPD) well
267 followed the T_a . The WD mainly followed the irrigation events in winter and spring, but
268 followed P in summer and autumn. In particular, the WD varied from 0 to 3 m throughout the
269 year. The wet soil conditions prohibited the field from experiencing water stress (Fig. 4d)
270 because even the lowest soil matric potential (-187.6 kPa) remained a lot higher than the

271 permanent wilting point of crops (around $-1, 500.0$ kPa).

272 **(Fig. 3&4 here)**

273 Fig. 5 shows the seasonal variations in H_C and PAI reflecting the crop development for the
274 full 2010-2011 cycle. The maximum PAI was $4.2 \text{ m}^2 \text{ m}^{-2}$ for wheat and $3.6 \text{ m}^2 \text{ m}^{-2}$ for maize.
275 The variations in H_C and PAI distinguished the different stages of crop development. During
276 the wheat season, the stages of regreening, jointing, booting, heading, and maturity started
277 approximately on March 1st, April 20th, May 1st, May 7th, and June 5th, respectively. The
278 seasonal variations in DM agreed well with the crop stages (Fig. 6), and the wheat biomass
279 mainly accumulated in April and May, while maize biomass mainly accumulated in July and
280 August. The total DM was $1, 718 \text{ g m}^{-2}$ for wheat and $1, 262 \text{ g m}^{-2}$ for maize at harvest. Upon
281 harvest, the wheat DM was distributed as: 3% root, 43% stem, 9% leaf and 45 % grain, while
282 the maize DM was distributed as: 2% root, 29% stem, 7% green leaf, 5% dead leaf, 4%
283 bracket, 7% cob, and 46% grain. The seasonal average carbon contents of the root, stem,
284 green leaf, dead leaf, and grain were 410, 439, 486, 452 and 457 gC kg^{-1} DM for wheat and,
285 408, 438, 477, 457, and 456 gC kg^{-1} DM for maize (see Table 1 for the seasonal variation).

286 **(Table 1 here)**

287 **(Figs. 5&6 here)**

288 **The inter-annual variations in the NEE, GPP and ER**

289 For the period from 2005 through 2016, if grain export was not considered, the wheat was
290 consistent CO_2 sink as the seasonal total NEEs were consistently negative, and the maize was
291 CO_2 sink in most years except for 2012 and 2013 when NEE was positive (Fig. 7a). NEEs of

292 both wheat and maize fields became less negative during the past decade (though not
293 statistically significant), implying a progressive decline of the carbon sequestration potential
294 of this cropland. The GPPs of both wheat and maize showed an increasing trend, though not
295 statistically significant (Fig. 7b). The ERs of both wheat and maize also showed an increasing
296 trend in these years, but only the trend of maize was significant (Fig. 7c). The decadal average
297 of NEE, GPP and ER were $-364 (\pm 98)$, $1,174 (\pm 189)$ and $810 (\pm 161)$ gC m⁻² for wheat,
298 and $-136 (\pm 168)$, $1,008 (\pm 297)$, and $872 (\pm 284)$ gC m⁻² for maize.

299 The NEE, GPP and ER for both wheat and maize were correlated with the three main
300 environmental variables of R_{si} , T_a and WD using the multiple regression (see Appendix B for
301 details). In the wheat season, T_a showed its relatively greater importance than R_{si} and WD to
302 all the three CO₂ fluxes with a higher T_a increasing both GPP and ER, and also enhancing
303 NEE (more negative) (Fig. 8a); WD correlated negatively with GPP, thereby reduced net
304 carbon uptake (less negative NEE); WD exhibited almost no effect on ER; R_{si} exhibited
305 almost no effect on all the three CO₂ fluxes. Therefore, T_a explained most of the inter-annual
306 variations in NEE, GPP and ER, followed by WD. In the maize season, WD had good
307 correlations with all the three fluxes of GPP, ER, and NEE, where a deeper WD contributed to
308 lower both GPP and ER, and also drive higher net carbon uptake (more negative NEE); T_a
309 showed almost no effect on all the three CO₂ fluxes; R_{si} had a positive correlation with ER,
310 but almost no correlation with GPP (Fig. 8b), ultimately, higher R_{si} in maize season lowered
311 the net carbon uptake (more positive NEE). Overall, R_{si} and WD showed their great
312 importance in influencing the inter-annual variation of maize NEE with R_{si} having a positive

313 correlation and WD having a comparable negative correlation (Fig. 8b).

314 (Figs. 7&8 here)

315 **Intra-annual variations in the NEE, GPP and ER**

316 The Intra-annual variations in NEE, GPP, and ER exhibited a bimodal curve corresponding
317 with the two crop seasons (Fig. 9). All the three CO₂ fluxes were almost in phase, with peaks
318 appearing at the start of May during the wheat season and in the middle of August during the
319 maize season. During some of the winter season, the field still sequestered a small amount of
320 CO₂ because of the weak photosynthesis, which was confirmed by leaf level gas exchange
321 measurement (data not shown). Net carbon emission happened during the fallow periods, in
322 addition to the start of the maize season when the plant was small and high temperature
323 enhanced heterotrophic respiration. During the wheat season, two evident spikes appeared on
324 April 21st and May 8th with positive NEE values (i.e., net carbon release). These spikes
325 resulted from the radiation decline during the inclement weather (Fig. 4b), which suppressed
326 the photosynthesis rate; similar phenomena also appeared during the maize season.

327 **(Fig. 9 here)**

328 Fig. 10 shows the variations in ER and its components. During the wheat season, the variation
329 in ER closely followed crop development and temperature, but there were two evident
330 declines at the end of April and the start of May due to low temperatures associated with the
331 inclement weather. During the early growing stage of maize, R_H was the main component of
332 ER. When water logging conditions occurred in late August and early September, both R_H and
333 R_{AB} were suppressed to zero.

334 (Fig. 10 here)

335 CO₂ budget synthesis in the 2010-2011 agricultural cycle

336 CO₂ budget analysis showed that this wheat-maize rotation cropland has the potential to
337 uptake carbon from the atmosphere (Fig. 11). In the full 2010-2011 cycle, the total NEE, GPP
338 and ER values were -438, 1078, and 640 gC m⁻² for wheat, and -239, 780 and 541 gC m⁻² for
339 maize. The NPP values were 750 and 815 gC m⁻² for wheat based on crop sample and the
340 eddy covariance complemented with soil respiration measurements, respectively, and were
341 592 and 532 gC m⁻² for maize based on the two methods. We used the average of these two
342 methods for NPP measurements, which were 783 (SD ± 46) gC m⁻² for wheat and 562 (SD ±
343 43) gC m⁻² for maize. We also used the average of NEP by two independent methods for the
344 measurement, and the NEP was 406 gC m⁻² for wheat and 269 gC m⁻² for maize. Furthermore,
345 when considering the carbon loss associated with the grain export, the NBP values were 59
346 gC m⁻² for wheat and 5 gC m⁻² for maize, respectively. Considering the net CO₂ loss of -104
347 gC m⁻² during the two fallow periods, NBP of the whole wheat-maize crop cycle was -40 gC
348 m⁻² yr⁻¹, suggesting that the cropland was a weak carbon source to the atmosphere under the
349 specific climatic conditions and field management practices.

350 (Fig. 11 here)

351 Discussion

352 This study investigated the decadal variations of the NEE, GPP and ER over an irrigated wheat-
353 maize rotation cropland over the North China Plain, and the results exhibited a decreasing trend
354 of the CO₂ sink capacity during the past decade. The inter-annual variations of the carbon fluxes

355 of wheat showed close dependence on temperature and groundwater depth, while those of maize
356 were mostly regulated by the solar radiation and groundwater depth. Furthermore, the detailed
357 CO₂ budget components were quantified for a full wheat-maize agricultural cycle. Investigating
358 the decadal trend of the CO₂ fluxes and quantifying the detailed CO₂ budget components for
359 this representative cropland will provide useful knowledge for the regional greenhouse gas
360 emission evaluation over the North China Plain.

361 **Comparison with other croplands**

362 The cropland has been reported as carbon neutral to the atmosphere (e.g., Ciais et al., 2010),
363 carbon source (e.g., Anthoni et al., 2004a; Verma et al., 2005; Kutsch et al., 2010; Wang et al.,
364 2015; Eichelmann et al., 2016), and also carbon sink (e.g., Kutsch et al., 2010). Such
365 inconsistency probably results from the different crop types and management practices
366 (residue removal, the use of organic manure etc), in addition to variations in the climatic
367 conditions (Béziat et al., 2009; Smith et al., 2014) and fallow period length (Dold et al.,
368 2017). Our results show that the fully irrigated wheat-maize rotation cropland with a shallow
369 groundwater depth was a weak CO₂ sink during both the wheat and maize seasons in the full
370 2010-2011 cycle, but the CO₂ loss during the fallow period reversed the cropland from a sink
371 into a weak source with an NBP of $-40 \text{ gC m}^{-2} \text{ yr}^{-1}$. These results are consistent with previous
372 studies that reported the wheat-maize rotation cropland as a carbon source (Li et al., 2006;
373 Wang et al., 2015). However, the net CO₂ loss was much lower at our site, most likely due to
374 the shallow groundwater depth.

375 Field measurements of the long term of CO₂ fluxes over croplands remain lacking, and we

376 found the carbon sequestration capacity of this cropland has been progressively decreasing.
377 The cropland has been widely suggested as a climate change mitigation tool (e.g., Lal, 2001),
378 but the potential in the future is challenging. However, since the cropland management greatly
379 impacts the carbon balance of cropland (Béziat et al., 2009; Ceschia et al., 2010), it remains
380 required investigating if the management adjustment can foster the cropland carbon sink
381 capacity over the long term.

382 The annual total NPP of 1,345 gC m⁻² yr⁻¹ at our site is approximately twice the average of
383 the model-estimated NPP for Chinese croplands (714 gC m⁻² yr⁻¹) with a rotation index of 2
384 (i.e., two crop cycles within one year) (Huang et al., 2007), more than three times the value
385 estimated by MODIS (400 gC m⁻² yr⁻¹) (Zhao et al., 2005), and slightly higher than the value
386 of the same crop rotation at the Luancheng site (1,144 gC m⁻² yr⁻¹) (Wang et al., 2015). The
387 higher NPP at our site may partially result from the sufficient irrigation and fertilization
388 (Huang et al., 2007; Smith et al., 2014).

389 The contrasting respiration partitionings of the same crop in different regions (Table 2)
390 indicate that the respiration processes may also be subject to climatic conditions and
391 management practices. Though the ecosystem respiration to GPP at our site is comparable to
392 other studies, the ratio of autotrophic respiration to GPP is much lower at our site, while the
393 ratio of heterotrophic respiration to ecosystem respiration is greater at our site, these findings
394 are different from those at the other sites with similar crop variety (Moureaux et al., 2008;
395 Aubinet et al., 2009; Suleau et al., 2011; Wang et al., 2015; Demyan et al., 2016), as they
396 showed that ecosystem respiration is usually dominated by below-ground and above-ground
397 autotrophic respirations. The higher soil heterotrophic respiration at our site probably results

398 from the full irrigation and shallow groundwater which alleviates soil water stress.

399 **(Table 2 here)**

400 **The effects of groundwater on carbon fluxes**

401 The groundwater table at our site is much closer to the surface because of the irrigation by
402 water diverted from the Yellow River, in contrast, the nearby Luancheng site (Wang et al.,
403 2015) is groundwater-fed with a very deep groundwater depth (approximately 42 m) (Shen et
404 al. 2013), and their CO₂ budget components had some difference with our study. Comparing
405 the net CO₂ exchange of wheat, the GPP at our site is a little higher than the Luancheng site,
406 implying the irrigation at our site may better sustain the photosynthesis rate for wheat; ER at
407 our site is also a little higher than Luancheng site. For maize, both sites are not irrigated due
408 to the high summer precipitation, GPP and ER at our site were comparable to Luancheng site,
409 implying that the irrigation method prior to the maize season had no discernible effect on the
410 integrated CO₂ fluxes for maize. However, the three components of ER in our study showed
411 pronounced difference from the Luancheng site, where they reported the R_{AA} was 411 gC m⁻²
412 for wheat and 428 gC m⁻² for maize, three times the results of our study (128 gC m⁻² for wheat
413 and 133 gC m⁻² for maize). However, their R_{AB} for wheat (36 gC m⁻²) and maize (16 gC m⁻²)
414 were less than a quarter of our results (136 gC m⁻² for wheat and 115 gC m⁻² for maize). Their
415 R_H of wheat (245 gC m⁻²) was less than our estimate (377 gC m⁻²), but R_H of maize (397 gC
416 m⁻²) was greater than our result (292 gC m⁻²). In general, the crop above-ground parts in our
417 site respired more carbon than the Luancheng site, possibly because the shallow groundwater
418 depth at our site increased the above-ground biomass allocation but lowered the root biomass

419 allocation (Poorter et al., 2012). These independent cross-site comparisons demonstrate that
420 carbon budget components may be subject to the specific groundwater depth influenced by
421 the irrigation type, and even the same crop under similar climatic conditions can behave
422 differently in carbon consumption.

423 Our site experienced a short period of water logging during the 2010-2011 cycle due to the
424 combined effects of full irrigation and the high precipitation during the summer. This distinct
425 field condition reduced soil carbon losses in the maize season, potentially maintaining the
426 CO₂ captured by the cropland. Water logging events were occasionally reported in upland
427 croplands, for example, Terazawa et al. (1992) and Iwasaki et al. (2010) suggested that water
428 logging causes damage to plants, resulting in a decline in GPP as reported by Dold et al.
429 (2017) and our study. Our study further shows that water logging reduces ER to a greater
430 degree than GPP possibly because of the low soil oxygen conditions, thereby reduces the
431 overall cropland CO₂ loss. However, the CH₄ release in the short period may be pronounced
432 in water-logged soils. As CH₄ emission in this kind of cropping system over the North China
433 Plain cropland remains lacking, additional field experiments are required to understand how
434 irrigation and water saturation field condition impact the overall carbon budget.

435 **Uncertainty in the estimation and limitation of this study**

436 In the comprehensive experiment period for the full 2010-2011 agricultural cycle, the NEE of
437 wheat season from October 23rd, 2010 to April 1st, 2011 was calculated using a calibrated
438 SVR model. The SVR model performs well in predicting GPP and ER with very high R² of
439 0.95 and 0.97 and an acceptable uncertainty level of 22.9% and 15.2% for GPP and ER,

440 respectively. Hence, these estimates should have a negligible effect on the seasonal total
441 carbon evaluation. The footprint analysis showed that 90% of the measured eddy flux comes
442 from the nearest 420 m and 166 m in wheat and maize crops under unstable conditions,
443 respectively, confirming that both soil respiration experiments and crop samples well paired
444 with the EC measurements.

445 Root biomass was difficult to measure, but the uncertainty should be low, because the root
446 ratio (the ratio of the root weight to the total biomass weight) accounts for 15-16 % of the
447 crop for wheat and maize (Wolf et al., 2015), and our measurements are very close to these
448 values, i.e., the averaged seasonal root ratio was 15% for wheat and 10% for maize at our
449 site. However, the relatively low root ratios (3% for wheat and 2% for maize) at harvest
450 probably result from the root decay associated with plant senescence. The estimates of annual
451 soil respiration are based on the Q_{10} model validated by the field measurements that may
452 generate some uncertainty in the soil respiration budget due to the hysteresis response of soil
453 respiration to temperature (Phillips et al., 2011; Zhang et al., 2015a; Zhang et al., 2018).
454 However, the Q_{10} model remains robust in soil respiration estimations if well validated (Tian
455 et al., 1999; Zhang et al., 2013; Latimer and Risk, 2016), allowing the confidence in the
456 estimates.

457 During the wheat season, the cumulative curves of NPP_{EC} and NPP_{CS} were not perfectly
458 consistent in the main growing season as clear differences emerged during the dormant season
459 of wheat from December 15th, 2010 to March 8th, 2011 (Fig. 12). These differences may result
460 from the small wheat sample number. However, the sample number at harvest was sufficiently

461 big and no discernible difference was found between the two NPPs at harvest. These two
462 independent estimates of NPP were similar throughout the maize season (Fig. 12).

463 This study provides a comprehensive quantification of the CO₂ budget components of the
464 cropland, but it remains limited to a relatively wet year (see Fig. 3c and d). The integrated
465 carbon fluxes (NEE, GPP and ER) have pronounced inter-annual variations, also suggesting
466 further investigations are required on the inter-annual variations of the carbon budget
467 components.

468 **(Fig. 12 here)**

469 **Conclusion**

470 Based on the decadal measurements of CO₂ fluxes over an irrigated wheat-maize rotation
471 cropland over the North China Plain, we found the cropland was a strong CO₂ sink if grain
472 export was not considered. When considering the grain export, the cropland was a weak CO₂
473 source with the NBP of $-40 \text{ gC m}^{-2} \text{ yr}^{-1}$ in the full 2010-2011 agricultural cycle. The net CO₂
474 exchange during the past decade from 2005 through 2016 showed a decreasing trend,
475 implying a decreasing carbon sequestration capacity of this cropland, discouraging the
476 potential of taking agro-ecosystems as the mitigation tool of climate change. In the wheat
477 season, air temperature showed the best correlation with the CO₂ fluxes followed by the
478 groundwater depth; while in the maize season, both short-wave radiation and groundwater
479 depth showed good correlation with the CO₂ fluxes. The comprehensive investigation showed
480 most of the carbon sequestration occurred during the wheat season, while maize was close to
481 being CO₂ neutral. Soil heterotrophic respiration in this cropland contributes substantially to

482 CO₂ loss in both wheat and maize season. This study provides detailed knowledge for
483 estimating regional carbon emission over the North China Plain.

484 **Appendix A. Flux calculation of the period with equipment failure**

485 A1. Support Vector Regression method

486 Support Vector Regression (SVR) method is a machine-learning technique-based regression,
487 which transforms regression from nonlinear into linear by mapping the original low-
488 dimensional input space to higher-dimensional space (Cristianini and Shave-Taylor, 2000).
489 SVR method has two advantages: 1) the model training always converges to global optimal
490 solution with only a few free parameters to adjust, and no experimentation is needed to
491 determine the architecture of SVR; 2) SVR method is robust to small errors in the training data
492 (Ueyama et al., 2013). The SVM software package obtained from LIBSVM (Chang and Lin,
493 2005) is used in this study.

494 A2. Data processing and selection of explanatory variables

495 Gross Primary Productivity (GPP) is influenced by several edaphic, atmospheric, and
496 physiological variables, among which air temperature (T_a), relative humidity (RH), plant area
497 index (PAI), net photosynthetically active radiation (PAR), and soil moisture (θ) are the
498 dominant factors. Hence, we select T_a , RH, PAI, PAR, and θ as explanatory variables of GPP.
499 Ecosystem Respiration (ER) consists of total soil respiration and above-ground autotrophic
500 respiration. The total soil respiration is largely influenced by soil temperature and soil moisture,
501 while above-ground autotrophic respiration is largely influenced by air temperature and above-
502 ground biomass. So we select T_a , soil temperature at 5 cm (T_s), θ and PAI as explanatory
503 variables of ER. PAI is estimated from the Wide Dynamic Range Vegetation Index derived from
504 the MOD09Q1 reflectance data (250 m, 8-d average,

505 https://lpdaac.usgs.gov/dataset_discovery/modis/modis_products_table/mod09q1, also see Lei
506 et al. 2013).

507 The three wheat seasons of 2005-2006, 2009-2010, and 2010-2011 are selected for model
508 training, and the original half-hourly measurements of GPP and ER together with the
509 explanatory variables are averaged to the daily scale, but we remove days missing more than
510 25% of half-hourly data. We have GPP available from 466 days and ER from 483 days for
511 model training. The explanatory variables for the equipment failure are also averaged into daily
512 scale, which will be used to calculate GPP and ER with the trained model described in the
513 following section.

514 A3. SVR model training and flux calculation

515 In order to eliminate the impact of variables with different absolute magnitudes, we rescale all
516 the variables in training-data set to the [0, 1] range prior to SVR model training. In the training
517 process, the radial basis function (RBF, a kernel function of SVR) is used and the width of
518 insensitive error band is set as 0.01. The SVR model training follows these steps:

519 (1) All training data samples are randomly divided into five non-overlapping subsets, and four
520 of them are selected as the training sets (also calibration set), the remaining subset is treated as
521 the test set (also validation set). Such process is repeated five times to ensure that every subset
522 has a chance to be the test set.

523 (2) For the selected training set, the SVR parameters (cost of errors c and kernel parameter σ)
524 are determined using a grid search with a five-fold cross-validation training process. In this
525 approach, the training set is further randomly divided into five non-overlapping subsets.

526 Training is performed on each of the four subsets within this training set, with the remaining
527 subset reserved for calculating the Root Mean Square Error (RMSE), and model parameters (c
528 and σ) yielding the minimum RMSE value are selected.

529 (3) The SVR model is trained based on the training set from step (1) and initialized by the
530 parameters (c and σ) derived from step (2).

531 (4) The test set from the step (1) is used to evaluate the model obtained from the step (3) by
532 using the coefficient of determination (R^2) and RMSE.

533 (5) The model is trained with all of the available samples with good performance achieved, as
534 R^2 are 0.95 and 0.97 for GPP and ER, respectively, and the mean RMSE are $1.28 \text{ gC m}^{-2} \text{ d}^{-1}$
535 and $0.44 \text{ gC m}^{-2} \text{ d}^{-1}$. The RMSE can be further used as a metric quantifying uncertainty, which
536 accounts for 22.9% and 15.2% for the averaged GPP and ER, respectively. GPP and ER during
537 equipment failure period are then calculated with the trained model complemented with the
538 observed explanatory variables, and NEE is derived as the difference of GPP and ER.

539 **Appendix B. Multiple regression for NEE, GPP and ER with microclimate variables**

540 The flux of NEE, GPP or ER is correlated with incoming short-wave radiation (R_{si}), air
541 temperature (T_a) and [groundwater depth](#) (WD) as $\text{flux} = aR_{si} + bT_a + cWD + d$, where flux is NEE,
542 GPP, or ER; a , b , c , and d are regression parameters. All the variables are normalized to derive
543 their z-score before the regression, where z-score is to subtract the mean from the data and
544 divide the result by standard deviation. The coefficient of each variable represents the relative
545 importance of the corresponding variable in contributing to the dependent variable.

546

547 **Data availability**

548 The data of this study are available for public after a request to the corresponding author.

549 **Author contributions**

550 Q.Z. and H.L. designed the study and methodology with substantial input from all co-authors. ,
551 Q.Z. conducted the field experiment. B.F. conducted the SVR calculation for gap filling. All
552 authors contributed to interpretation of the results. Q.Z. drafted the manuscript, and all authors
553 edited and approved the final manuscript.

554 **Competing interests**

555 The authors declare that they have no conflict of interest.

556 **Acknowledgement**

557 This research was supported by the NSFC-NSF collaboration (P. R. China-U.S.) funding (No.
558 51861125102), National Natural Science Foundation of China (Project Nos. 51509187,
559 51679120 and 51525902).

560 **Reference**

561 Anthoni, P. M., Freibauer, A., Kolle, O., and Schulze, E. D.: Winter wheat carbon exchange in
562 Thuringia, Germany, *Agric. For. Meteorol.*, 121, 55-67, doi: 10.1016/s0168-1923(03)00162-
563 x, 2004a.

564 Anthoni, P. M., Knohl, A., Rebmann, C., Freibauer, A., Mund, M., Ziegler, W., Kolle, O., and
565 Schulze, E. D.: Forest and agricultural land-use-dependent CO₂ exchange in Thuringia,
566 Germany, *Global Change Biol.*, 10, 2005-2019, doi: 10.1111/j.1365-2486.2004.00863.x,
567 2004b.

568 Aubinet, M., Grelle, A., Ibrom, A., Rannik, Ü., Moncrieff, J., Foken, T., Kowalski, A. S.,

569 Martin, P. H., Berbigier, P., Bernhofer, C., Clement, R., Elbers, J., Granier, A., Grunwald,
570 T., Morgenstern, K., Pilegaard, K., Rebmann, C., Snijders, W., Valentini, R., and Vesala, T.:
571 Estimates of the annual net carbon and water exchange of forests: The EUROFLUX
572 methodology, *Adv. Ecol. Res.*, 30, 113-175, 2000.

573 Aubinet, M., Moureaux, C., Bodson, B., Dufranne, D., Heinesch, B., Suleau, M., Vancutsem,
574 F., and Vilret, A.: Carbon sequestration by a crop over a 4-year sugar beet/winter wheat/seed
575 potato/winter wheat rotation cycle, *Agric. For. Meteorol.*, 149, 407-418, doi:
576 10.1016/j.agrformet.2008.09.003, 2009.

577 Baker, J. M., and Griffis, T. J.: Examining strategies to improve the carbon balance of
578 corn/soybean agriculture using eddy covariance and mass balance techniques, *Agric. For.*
579 *Meteorol.*, 128, 163-177, doi: 10.1016/j.agrformet.2004.11.005, 2005.

580 Baldocchi, D., Falge, E., Gu, L. H., Olson, R., Hollinger, D., Running, S., Anthoni, P.,
581 Bernhofer, C., Davis, K., Evans, R., Fuentes, J., Goldstein, A., Katul, G., Law, B., Lee, X.
582 H., Malhi, Y., Meyers, T., Munger, W., Oechel, W., U, K. T. P., Pilegaard, K., Schmid, H.
583 P., Valentini, R., Verma, S., Vesala, T., Wilson, K., and Wofsy, S.: FLUXNET: A new tool
584 to study the temporal and spatial variability of ecosystem-scale carbon dioxide, water vapor,
585 and energy flux densities, *B Am. Meteorol. Soc.*, 82, 2415-2434, 2001.

586 Béziat, P., Ceschia, E., and Dedieu, G.: Carbon balance of a three crop succession over two
587 cropland sites in South West France, *Agric. For. Meteorol.*, 149, 1628-1645, doi:
588 10.1016/j.agrformet.2009.05.004, 2009.

589 Bondeau, A., Smith, P. C., Zaehle, S., Schaphoff, S., Lucht, W., Cramer, W., Gerten, D., Lotze-

590 Campen, H., Muller, C., Reichstein, M., and Smith, B.: Modelling the role of agriculture for
591 the 20th century global terrestrial carbon balance, *Global Change Biol.*, 13, 679-706, doi:
592 10.1111/j.1365-2486.2006.01305.x, 2007.

593 Cao, G., Scanlon, B.R., Han, D. and Zheng, C.: Impacts of thickening unsaturated zone on
594 groundwater recharge in the North China Plain. *J. Hydrol.*, 537, 260-270, doi:
595 10.1016/j.jhydrol.2016.03.049, 2016.

596 Ceschia, E., Béziat, P., Dejoux, J. F., Aubinet, M., Bernhofer, C., Bodson, B., Buchmann, N.,
597 Carrara, A., Cellier, P., Di Tommasi, P., Elbers, J. A., Eugster, W., Grunwald, T., Jacobs, C.
598 M. J., Jans, W. W. P., Jones, M., Kutsch, W., Lanigan, G., Magliulo, E., Marloie, O., Moors,
599 E. J., Moureaux, C., Olioso, A., Osborne, B., Sanz, M. J., Saunders, M., Smith, P., Soegaard,
600 H., and Wattenbach, M.: Management effects on net ecosystem carbon and GHG budgets at
601 European crop sites, *Agric. Ecosyst. Environ.*, 139, 363-383, doi:
602 10.1016/j.agee.2010.09.020, 2010.

603 Chang, C. C., and Lin, C. J.: LIBSVM-A library for Support Vector Machines.
604 <http://www.csie.ntu.edu.tw/~cjlin/libsvm/>, 2005.

605 Chen, Y. L., Luo, G. P., Maisupova, B., Chen, X., Mukanov, B. M., Wu, M., Mambetov, B. T.,
606 Huang, J. F., and Li, C. F.: Carbon budget from forest land use and management in Central
607 Asia during 1961-2010, *Agric. For. Meteorol.*, 221, 131-141, doi:
608 10.1016/j.agrformet.2016.02.011, 2016.

609 Ciais, P., Wattenbach, M., Vuichard, N., Smith, P., Piao, S. L., Don, A., Luysaert, S., Janssens,
610 I. A., Bondeau, A., Dechow, R., Leip, A., Smith, P. C., Beer, C., van der Werf, G. R., Gervois,

611 S., Van Oost, K., Tomelleri, E., Freibauer, A., Schulze, E. D., and Team, C. S.: The European
612 carbon balance. Part 2: croplands, *Global Change Biol.*, 16, 1409-1428, doi: 10.1111/j.1365-
613 2486.2009.02055.x, 2010.

614 Ciais, P., Gervois, S., Vuichard, N., Piao, S. L., and Viovy, N.: Effects of land use change and
615 management on the European cropland carbon balance, *Global Change Biol.*, 17, 320-338,
616 doi: 10.1111/j.1365-2486.2010.02341.x, 2011.

617 Cristianini, N., and Shawe-Taylor, J.: *An Introduction to Support Vector Machines and Other*
618 *Kernel-Based Learning Methods*, Cambridge Univ. Press, Cambridge, UK, pp. 189, 2000.

619 Demyan, M. S., Ingwersen, J., Funkuin, Y. N., Ali, R. S., Mirzaeitalarposhti, R., Rasche, F.,
620 Poll, C., Muller, T., Streck, T., Kandeler, E., and Cadisch, G.: Partitioning of ecosystem
621 respiration in winter wheat and silage maize-modeling seasonal temperature effects, *Agric.*
622 *Ecosyst. Environ.*, 224, 131-144, doi: 10.1016/j.agee.2016.03.039, 2016.

623 de la Motte, L. G., Jérôme, E., Mamadou, O., Beckers, Y., Bodson, B., Heinesch, B., and
624 Aubinet, M.: Carbon balance of an intensively grazed permanent grassland in southern
625 Belgium, *Agric. For. Meteorol.*, 228-229, 370-383, doi: 10.1016/j.agrformet.2016.06.009,
626 2016.

627 Dold, C., Büyükcangaz, H., Rondinelli, W., Prueger, J., Sauer, T., and Hatfield, J.: Long-term
628 carbon uptake of agro-ecosystems in the Midwest, *Agric. For. Meteorol.*, 232, 128-140, doi:
629 10.1016/j.agrformet.2016.07.012, 2017.

630 Drewniak, B. A., Mishra, U., Song, J., Prell, J., and Kotamarthi, V. R.: Modeling the impact of
631 agricultural land use and management on US carbon budgets, *Biogeosciences*, 12, 2119-
632 2129, doi: 10.5194/bg-12-2119-2015, 2015.

633 Eichelmann, E., Wagner-Riddle, C., Warland, J., Deen, B., and Voroney, P.: Comparison of
634 carbon budget, evapotranspiration, and albedo effect between the biofuel crops switchgrass
635 and corn, *Agric. Ecosyst. Environ.*, 231, 271-282, doi: 10.1016/j.agee.2016.07.007, 2016.

636 Ekblad, A., Bostrom, B., Holm, A., and Comstedt, D.: Forest soil respiration rate and $\delta^{13}\text{C}$ is
637 regulated by recent above ground weather conditions, *Oecologia*, 143, 136-142, doi:
638 10.1007/s00442-004-1776-z, 2005.

639 Eugster, W., Moffat, A. M., Ceschia, E., Aubinet, M., Ammann, C., Osborne, B., Davis, P. A.,
640 Smith, P., Jacobs, C., Moors, E., Le Dantec, V., Beziat, P., Saunders, M., Jans, W., Grunwald,
641 T., Rebmann, C., Kutsch, W. L., Czerny, R., Janous, D., Moureaux, C., Dufranne, D., Carrara,
642 A., Magliulo, V., Di Tommasi, P., Olesen, J. E., Schelde, K., Oliosio, A., Bernhofer, C.,
643 Cellier, P., Larmanou, E., Loubet, B., Wattenbach, M., Marloie, O., Sanz, M. J., Sogaard,
644 H., and Buchmann, N.: Management effects on European cropland respiration, *Agric.*
645 *Ecosyst. Environ.*, 139, 346-362, doi: 10.1016/j.agee.2010.09.001, 2010.

646 Falkowski, P., Scholes, R. J., Boyle, E. E. A., Canadell, J., Canfield, D., Elser, J., Gruber, N.,
647 Hibbard, K., Högberg, P., Linder, S., and Mackenzie, F. T.: The global carbon cycle: a test
648 of our knowledge of earth as a system, *Science*, 290, 291-296, doi:
649 10.1126/science.290.5490.291, 2000.

650 Falge, E., Baldocchi, D., Olson, R., Anthoni, P., Aubinet, M., Bernhofer, C., Burba, G.,
651 Ceulemans, R., Clement, R., Dolman, H., Granier, A., Gross, P., Grunwald, T., Hollinger,
652 D., Jensen, N. O., Katul, G., Keronen, P., Kowalski, A., Lai, C. T., Law, B. E., Meyers, T.,
653 Moncrieff, H., Moors, E., Munger, J. W., Pilegaard, K., Rannik, U., Rebmann, C., Suyker,
654 A., Tenhunen, J., Tu, K., Verma, S., Vesala, T., Wilson, K., and Wofsy, S.: Gap filling

655 strategies for defensible annual sums of net ecosystem exchange, *Agric. For. Meteorol.*, 107,
656 43-69, doi: 10.1016/S0168-1923(00)00225-2, 2001.

657 Falge, E., Baldocchi, D., Tenhunen, J., Aubinet, M., Bakwin, P., Berbigier, P., Bernhofer, C.,
658 Burba, G., Clement, R., Davis, K. J., Elbers, J. A., Goldstein, A. H., Grelle, A., Granier, A.,
659 Guomundsson, J., Hollinger, D., Kowalski, A. S., Katul, G., Law, B. E., Malhi, Y., Meyers,
660 T., Monson, R. K., Munger, J. W., Oechel, W., Paw, K. T., Pilegaard, K., Rannik, U.,
661 Rebmann, C., Suyker, A., Valentini, R., Wilson, K., and Wofsy, S.: Seasonality of ecosystem
662 respiration and gross primary production as derived from FLUXNET measurements, *Agric.*
663 *For. Meteorol.*, 113, 53-74, doi: 10.1016/S0168-1923(02)00102-8, 2002a.

664 Falge, E., Tenhunen, J., Baldocchi, D., Aubinet, M., Bakwin, P., Berbigier, P., Bernhofer, C.,
665 Bonnefond, J. M., Burba, G., Clement, R., Davis, K. J., Elbers, J. A., Falk, M., Goldstein, A.
666 H., Grelle, A., Granier, A., Grunwald, T., Gudmundsson, J., Hollinger, D., Janssens, I. A.,
667 Keronen, P., Kowalski, A. S., Katul, G., Law, B. E., Malhi, Y., Meyers, T., Monson, R. K.,
668 Moors, E., Munger, J. W., Oechel, W., U, K. T. P., Pilegaard, K., Rannik, U., Rebmann, C.,
669 Suyker, A., Thorgeirsson, H., Tirone, G., Turnipseed, A., Wilson, K., and Wofsy, S.: Phase
670 and amplitude of ecosystem carbon release and uptake potentials as derived from FLUXNET
671 measurements, *Agric. For. Meteorol.*, 113, 75-95, doi: 10.1016/S0168-1923(02)00103-X,
672 2002b.

673 Fargione, J. E., Bassett, S., Boucher, T., Bridgham, S. D., Conant, R. T., Cook-Patton, S. C.,
674 Ellis, P. W., Falcucci, A., Fourqurean, J. W., Gopalakrishna, T., Gu, H., Henderson, B.,
675 Hurteau, M. D., Kroeger, K. D., Kroeger, T., Lark, T. J., Leavitt, S. M., Lomax, G.,
676 McDonald, R. I., Megonigal, J. P., Miteva, D. A., Richardson, C. J., Sanderman, J., Shoch,

677 D., Spawn, S. A., Veldman, J. W., Williams, C. A., Woodbury, P. B., Zganjar, C., Baranski,
678 M., Elias, P., Houghton, R. A., Landis, E., McGlynn, E., Schlesinger, W. H., Siikamaki, J.
679 V., Sutton-Grier, A. E., and Griscom, B. W.: Natural climate solutions for the United States,
680 *Sci Adv*, 4, doi: 10.1126/sciadv.aat1869, 2018.

681 Fleisher, D. H., Timlin, D. J., and Reddy, V. R.: Elevated carbon dioxide and water stress effects
682 on potato canopy gas exchange, water use, and productivity, *Agric. For. Meteorol.*, 148,
683 1109-1122, doi: 10.1016/j.agrformet.2008.02.007, 2008.

684 Forkel, M., Carvalhais, N., Rödenbeck, C., Keeling, R., Heimann, M., Thonicke, K., Zaehle, S.,
685 and Reichstein, M.: Enhanced seasonal CO₂ exchange caused by amplified plant productivity
686 in northern ecosystems, *Science*, 351, 696-699, doi: 10.1126/science.aac4971, 2016.

687 Freibauer, A., Rounsevell, M. D. A., Smith, P., and Verhagen, J.: Carbon sequestration in the
688 agricultural soils of Europe, *Geoderma*, 122, 1-23, 10.1016/j.geoderma.2004.01.021, 2004.

689 Gao, X., Gu, F., Hao, W., Mei, X., Li, H., Gong, D., and Zhang, Z.: Carbon budget of a rainfed
690 spring maize cropland with straw returning on the Loess Plateau, China, *Science of The Total*
691 *Environment*, 586, 1193-1203, 10.1016/j.scitotenv.2017.02.113, 2017.

692 Gilmanov, T. G., Verma, S. B., Sims, P. L., Meyers, T. P., Bradford, J. A., Burba, G. G., and
693 Suyker, A. E.: Gross primary production and light response parameters of four Southern
694 Plains ecosystems estimated using long-term CO₂-flux tower measurements, *Global*
695 *Biogeochem. Cycles*, 17, Artn 1071, doi: 10.1029/2002gb002023, 2003.

696 Grant, R. F., Arkebauer, T. J., Dobermann, A., Hubbard, K. G., Schimelfenig, T. T., Suyker, A.
697 E., Verma, S. B., and Walters, D. T.: Net biome productivity of irrigated and rainfed maize-
698 soybean rotations: Modeling vs. measurements, *Agron. J.*, 99, 1404-1423, doi:

699 10.2134/agronj2006.0308, 2007.

700 Gray, J. M., Frohking, S., Kort, E. A., Ray, D. K., Kucharik, C. J., Ramankutty, N., and Friedl,
701 M. A.: Direct human influence on atmospheric CO₂ seasonality from increased cropland
702 productivity, *Nature*, 515, 398-401, doi: 10.1038/nature13957, 2014.

703 Griscom, B. W., Adams, J., Ellis, P. W., Houghton, R. A., Lomax, G., Miteva, D. A., Schlesinger,
704 W. H., Shoch, D., Siikamaki, J. V., Smith, P., Woodbury, P., Zganjar, C., Blackman, A.,
705 Campari, J., Conant, R. T., Delgado, C., Elias, P., Gopalakrishna, T., Hamsik, M. R., Herrero,
706 M., Kiesecker, J., Landis, E., Laestadius, L., Leavitt, S. M., Minnemeyer, S., Polasky, S.,
707 Potapov, P., Putz, F. E., Sanderman, J., Silvius, M., Wollenberg, E., and Fargione, J.: Natural
708 climate solutions, *P. Natl. Acad. Sci. USA*, 114, 11645-11650, doi:
709 10.1073/pnas.1710465114, 2017.

710 Heimann, M., and Reichstein, M.: Terrestrial ecosystem carbon dynamics and climate
711 feedbacks, *Nature*, 451, 289-292, doi: 10.1038/Nature06591, 2008.

712 Hollinger, S. E., Bernacchi, C. J., and Meyers, T. P.: Carbon budget of mature no-till ecosystem
713 in North Central Region of the United States, *Agric. For. Meteorol.*, 130, 59-69, doi:
714 10.1016/j.agrformet.2005.01.005, 2005.

715 Hsieh, C. I., Katul, G., and Chi, T.: An approximate analytical model for footprint estimation
716 of scalar fluxes in thermally stratified atmospheric flows, *Adv. Water Resour*, 23, 765-772,
717 doi: 10.1016/S0309-1708(99)00042-1, 2000.

718 Huang, Y., Zhang, W., Sun, W. J., and Zheng, X. H.: Net primary production of Chinese
719 croplands from 1950 to 1999, *Ecol. Appl.*, 17, 692-701, doi: 10.1890/05-1792, 2007.

720 Hunt, J. E., Laubach, J., Barthel, M., Fraser, A., and Phillips, R. L.: Carbon budgets for an

721 irrigated intensively grazed dairy pasture and an unirrigated winter-grazed pasture,
722 Biogeosciences, 13, 2927-2944, doi: 10.5194/bg-13-2927-2016, 2016.

723 Hutchinson, J. J., Campbell, C. A., and Desjardins, R. L.: Some perspectives on carbon
724 sequestration in agriculture, Agric. For. Meteorol., 142, 288-302, doi:
725 10.1016/j.agrformet.2006.03.030, 2007.

726 Iwasaki, H., Saito, H., Kuwao, K., Maximov, T. C., and Hasegawa, S.: Forest decline caused
727 by high soil water conditions in a permafrost region, Hydrol. Earth Syst. Sc., 14, 301-307,
728 doi: 10.5194/hess-14-301-2010, 2010.

729 Jans, W. W. P., Jacobs, C. M. J., Kruijt, B., Elbers, J. A., Barendse, S., and Moors, E. J.: Carbon
730 exchange of a maize (*Zea mays* L.) crop: Influence of phenology, Agric. Ecosyst. Environ.,
731 139, 316-324, doi: 10.1016/j.agee.2010.06.008, 2010.

732 Kang, M., Ichii, K., Kim, J., Indrawati, Y. M., Park, J., Moon, M., Lim, J. H., and Chun, J. H.:
733 New gap-filling strategies for long-period flux data gaps using a data-driven approach,
734 Atmosphere-Basel, 10, doi: 10.3390/Atmos10100568, 2019.

735 Kendy, E., Gerard-Marchant, P., Walter, M. T., Zhang, Y. Q., Liu, C. M., and Steenhuis, T. S.:
736 A soil-water-balance approach to quantify groundwater recharge from irrigated cropland in
737 the North China Plain, Hydrol. Process., 17, 2011-2031, doi: 10.1002/hyp.1240, 2003.

738 Kim, Y., Johnson, M.S., Knox, S.H., Black, T. A., Dalmagro, H. J., Kang, M., Kim, J.,
739 Baldocchi, D.: Gap-filling approaches for eddy covariance methane fluxes: A comparison of
740 three machine learning algorithms and a traditional method with principal component
741 analysis. Global Change Biol., 26, 1-20 doi: 10.1111/gcb.14845, 2019.

742 Kutsch, W. L., Aubinet, M., Buchmann, N., Smith, P., Osborne, B., Eugster, W., Wattenbach,

743 M., Schrumpf, M., Schulze, E. D., Tomelleri, E., Ceschia, E., Bernhofer, C., Beziat, P.,
744 Carrara, A., Di Tommasi, P., Grunwald, T., Jones, M., Magliulo, V., Marloie, O., Moureaux,
745 C., Oliosio, A., Sanz, M. J., Saunders, M., Sogaard, H., and Ziegler, W.: The net biome
746 production of full crop rotations in Europe, *Agric. Ecosyst. Environ.*, 139, 336-345, doi:
747 10.1016/j.agee.2010.07.016, 2010.

748 Lal, R.: World cropland soils as a source or sink for atmospheric carbon, *Adv. Agron.*, 71, 145-
749 191, 2001.

750 Latimer, R. N. C. and Risk, D. A.: An inversion approach for determining distribution of
751 production and temperature sensitivity of soil respiration, *Biogeosciences*, 13, 2111-2122,
752 doi: 10.5194/bg-13-2111-2016, 2016.

753 Lei, H. M., and Yang, D. W.: Seasonal and interannual variations in carbon dioxide exchange
754 over a cropland in the North China Plain, *Global Change Biol.*, 16, 2944-2957, doi:
755 10.1111/j.1365-2486.2009.02136.x, 2010.

756 Lei, H. M., Yang, D. W., Cai, J. F., and Wang, F. J.: Long-term variability of the carbon balance
757 in a large irrigated area along the lower Yellow River from 1984 to 2006, *Sci. China Earth*
758 *Sci.*, 56, 671-683, doi: 10.1007/s11430-012-4473-5, 2013.

759 Li, J., Yu, Q., Sun, X. M., Tong, X. J., Ren, C. Y., Wang, J., Liu, E. M., Zhu, Z. L., and Yu, G.
760 R.: Carbon dioxide exchange and the mechanism of environmental control in a farmland
761 ecosystem in North China Plain, *Sci. China Ser. D*, 49, 226-240, doi: 10.1007/s11430-006-
762 8226-1, 2006.

763 Luo, Y., He, C. S., Sophocleous, M., Yin, Z. F., Ren, H. R., and Zhu, O. Y.: Assessment of
764 crop growth and soil water modules in SWAT2000 using extensive field experiment data in

765 an irrigation district of the Yellow River Basin, *J Hydrol*, 352, 139-156, doi:
766 10.1016/j.jhydrol.2008.01.003, 2008.

767 Mauder, M., and Foken, T.: Documentation and instruction manual of the eddy covariance
768 software package TK2. Universität Bayreuth, Abt. Mikrometeorologie, Arbeitsergebnisse,
769 2004.

770 Mauder, M., and Foken, T.: Documentation and instruction manual of the eddy-covariance
771 software package TK3, Universität Bayreuth, Abt. Mikrometeorologie, Arbeitsergebnisse
772 2011.

773 Moureaux, C., Debacq, A., Bodson, B., Heinesch, B., and Aubinet, M.: Annual net ecosystem
774 carbon exchange by a sugar beet crop, *Agric. For. Meteorol.*, 139, 25-39, doi:
775 10.1016/j.agrformet.2006.05.009, 2006.

776 Moureaux, C., Debacq, A., Hoyaux, J., Suleau, M., Tourneur, D., Vancutsem, F., Bodson, B.,
777 and Aubinet, M.: Carbon balance assessment of a Belgian winter wheat crop (*Triticum*
778 *aestivum* L.), *Global Change Biol.*, 14, 1353-1366, doi: 10.1111/j.1365-2486.2008.01560.x,
779 2008.

780 National Standards of Environmental Protection of the People's Republic of China: Soil –
781 Determination of organic carbon – Combustion oxidation-titration method. HJ658-2013,
782 2013.

783 Özdoğan, M.: Exploring the potential contribution of irrigation to global agricultural primary
784 productivity, *Global Biogeochem. Cycles*, 25, doi: 10.1029/2009GB003720, 2011.

785 Phillips, C. L., Nickerson, N., Risk, D. and Bond, B. J.: Interpreting diel hysteresis between soil
786 respiration and temperature, *Global Change Biol.*, 17, 515-527, doi: 10.1111/j.1365-

787 2486.2010.02250.x, 2011.

788 Piao, S. L., Ito, A., Li, S. G., Huang, Y., Ciais, P., Wang, X. H., Peng, S. S., Nan, H. J., Zhao,
789 C., Ahlstrom, A., Andres, R. J., Chevallier, F., Fang, J. Y., Hartmann, J., Huntingford, C.,
790 Jeong, S., Levis, S., Levy, P. E., Li, J. S., Lomas, M. R., Mao, J. F., Mayorga, E., Mohammat,
791 A., Muraoka, H., Peng, C. H., Peylin, P., Poulter, B., Shen, Z. H., Shi, X., Sitch, S., Tao, S.,
792 Tian, H. Q., Wu, X. P., Xu, M., Yu, G. R., Viovy, N., Zaehle, S., Zeng, N., and Zhu, B.: The
793 carbon budget of terrestrial ecosystems in East Asia over the last two decades,
794 *Biogeosciences*, 9, 3571-3586, doi: 10.5194/bg-9-3571-2012, 2012.

795 [Poorter, H., Niklas, K. J., Reich, P. B., Oleksyn, J., Poot, P., and Mommer, L.: Biomass](#)
796 [allocation to leaves, stems and roots: meta-analyses of interspecific variation and](#)
797 [environmental control, *New Phytol*, 193, 30-50, doi: 10.1111/j.1469-8137.2011.03952.x,](#)
798 [2012.](#)

799 Poulter, B., Frank, D., Ciais, P., Myneni, R. B., Andela, N., Bi, J., Broquet, G., Canadell, J. G.,
800 Chevallier, F., Liu, Y. Y. and Running, S. W.: Contribution of semi-arid ecosystems to
801 interannual variability of the global carbon cycle, *Nature*, 509, 600-603,
802 doi:10.1038/nature13376, 2014.

803 Reichstein, M., Falge, E., Baldocchi, D., Papale, D., Aubinet, M., Berbigier, P., Bernhofer, C.,
804 Buchmann, N., Gilmanov, T., Granier, A., Grunwald, T., Havrankova, K., Ilvesniemi, H.,
805 Janous, D., Knohl, A., Laurila, T., Lohila, A., Loustau, D., Matteucci, G., Meyers, T.,
806 Miglietta, F., Ourcival, J. M., Pumpanen, J., Rambal, S., Rotenberg, E., Sanz, M., Tenhunen,
807 J., Seufert, G., Vaccari, F., Vesala, T., Yakir, D., and Valentini, R.: On the separation of net
808 ecosystem exchange into assimilation and ecosystem respiration: review and improved

809 algorithm, *Global Change Biol.*, 11, 1424-1439, doi: 10.1111/j.1365-2486.2005.001002.x,
810 2005.

811 Sauerbeck, D. R.: CO₂ emissions and C sequestration by agriculture - perspectives and
812 limitations, *Nutr. Cycl. Agroecosys.*, 60, 253-266, doi: 10.1023/A:1012617516477, 2001.

813 Schmidt, M., Reichenau, T. G., Fiener, P., and Schneider, K.: The carbon budget of a winter
814 wheat field: An eddy covariance analysis of seasonal and inter-annual variability, *Agric. For.
815 Meteorol.*, 165, 114-126, doi: 10.1016/j.agrformet.2012.05.012, 2012.

816 Shen, Y., Zhang, Y., Scanlon, B. R., Lei, H., Yang, D., and Yang, F: Energy/water budgets and
817 productivity of the typical croplands irrigated with groundwater and surface water in the
818 North China Plain, *Agric. For. Meteorol.*, 181, 133-142, doi:
819 10.1016/j.agrformet.2013.07.013, 2013.

820 Smith, P.: Carbon sequestration in croplands: the potential in Europe and the global context,
821 *Eur. J. Agron.*, 20, 229-236, doi: 10.1016/j.eja.2003.08.002, 2004.

822 Smith, P., Lanigan, G., Kutsch, W. L., Buchmann, N., Eugster, W., Aubinet, M., Ceschia, E.,
823 Beziat, P., Yeluripati, J. B., Osborne, B., Moors, E. J., Brut, A., Wattenbach, M., Saunders,
824 M., and Jones, M.: Measurements necessary for assessing the net ecosystem carbon budget
825 of croplands, *Agric. Ecosyst. Environ.*, 139, 302-315, doi: 10.1016/j.agee.2010.04.004, 2010.

826 Smith, W. K., Cleveland, C. C., Reed, S. C., and Running, S. W.: Agricultural conversion
827 without external water and nutrient inputs reduces terrestrial vegetation productivity,
828 *Geophys. Res. Lett.*, 41, 449-455, doi: 10.1002/2013GL058857, 2014.

829 Suyker, A.E., Verma, S. B., Burba, G. G., and Arkebauer, T. J., Gross primary production and
830 ecosystem respiration of irrigated maize and irrigated soybean during a growing season.

831 Agric. For. Meteorol., 31, 180-190, doi: 10.1016/j.agrformet.2005.05.007, 2005.

832 Suleau, M., Moureaux, C., Dufranne, D., Buysse, P., Bodson, B., Destain, J. P., Heinesch, B.,
833 Debacq, A., and Aubinet, M.: Respiration of three Belgian crops: Partitioning of total
834 ecosystem respiration in its heterotrophic, above- and below-ground autotrophic components,
835 Agric. For. Meteorol., 151, 633-643, doi: 10.1016/j.agrformet.2011.01.012, 2011.

836 Taylor, A. M., Amiro, B. D., and Fraser, T. J.: Net CO₂ exchange and carbon budgets of a three-
837 year crop rotation following conversion of perennial lands to annual cropping in Manitoba,
838 Canada, Agric. For. Meteorol., 182–183, 67-75, doi: 10.1016/j.agrformet.2013.07.008, 2013.

839 Terazawa, K., Maruyama, Y., and Morikawa, Y.: Photosynthetic and Stomatal Responses of
840 Larix-Kaempferi Seedlings to Short-Term Waterlogging, Ecol. Res., 7, 193-197, doi:
841 10.1007/Bf02348500, 1992.

842 Tian, H., Melillo, J., Kicklighter, D., McGuire, A., and Helfrich, J.: The sensitivity of terrestrial
843 carbon storage to historical climate variability and atmospheric CO₂ in the United States,
844 Tellus B, 51, 414-452, 1999.

845 Ueyama, M., Ichii, K., Iwata, H., Euskirchen, E. S., Zona, D., Rocha, A. V., Harazono, Y.,
846 Iwama, C., Nakai, T., and Oechel, W. C.: Upscaling terrestrial carbon dioxide fluxes in
847 Alaska with satellite remote sensing and support vector regression, J. Geophys. Res-Bioge.,
848 118, 1266-1281, doi: 10.1002/jgrg.20095, 2013.

849 van Wesemael, B., Paustian, K., Meersmans, J., Goidts, E., Barancikova, G., and Easter, M.:
850 Agricultural management explains historic changes in regional soil carbon stocks, P. Natl.
851 Acad. Sci. USA, 107, 14926-14930, doi: 10.1073/pnas.1002592107, 2010.

852 Verma, S. B., Dobermann, A., Cassman, K. G., Walters, D. T., Knops, J. M., Arkebauer, T. J.,

853 Suyker, A. E., Burba, G. G., Amos, B., Yang, H. S., Ginting, D., Hubbard, K. G., Gitelson,
854 A. A., and Walter-Shea, E. A.: Annual carbon dioxide exchange in irrigated and rainfed
855 maize-based agroecosystems, *Agric. For. Meteorol.*, 131, 77-96, doi:
856 10.1016/j.agrformet.2005.05.003, 2005.

857 Vick, E. S. K., Stoy, P. C., Tang, A. C. I., and Gerken, T.: The surface-atmosphere exchange of
858 carbon dioxide, water, and sensible heat across a dryland wheat-fallow rotation, *Agric.*
859 *Ecosyst. Environ.*, 232,129-140, doi: 10.1016/j.agee.2016.07.018, 2016.

860 Wang, Y. Y., Hu, C. S., Dong, W. X., Li, X. X., Zhang, Y. M., Qin, S. P., and Oenema, O.:
861 Carbon budget of a winter-wheat and summer-maize rotation cropland in the North China
862 Plain, *Agric. Ecosyst. Environ.*, 206, 33-45, doi: 10.1016/j.agee.2015.03.016, 2015.

863 [Wolf, J., West, T. O., Le Page, Y., Kyle, G. P., Zhang, X., Collatz, G. J., and Imhoff, M. L.:](#)
864 [Biogenic carbon fluxes from global agricultural production and consumption, *Global*](#)
865 [Biogeochem. Cy.](#), 29, 1617-1639, doi: 10.1002/2015gb005119, 2015.

866 Zhang, Q., Lei, H. M., and Yang, D. W.: Seasonal variations in soil respiration, heterotrophic
867 respiration and autotrophic respiration of a wheat and maize rotation cropland in the North
868 China Plain, *Agric. For. Meteorol.*, 180, 34-43, doi: 10.1016/j.agrformet.2013.04.028, 2013.

869 Zhang, Q., Katul, G. G., Oren, R., Daly, E., Manzoni, S., and Yang, D. W.: The hysteresis
870 response of soil CO₂ concentration and soil respiration to soil temperature, *J. Geophys. Res-*
871 *Biogeo.*, 120, 1605-1618, doi: 10.1002/2015JG003047, 2015a.

872 Zhang, Q., Lei, H.M., Yang, D.W., Bo H. B., and Cai, J. F.: On the diel characteristics of soil
873 respiration over the North China Plain, *J. Tsinghua University (Science and Technology)*,
874 55, 33-38, 2015b. (in Chinese with English abstract)

875 Zhang, Q., Phillips, R.P., Manzoni, S., Scott, R.L., Oishi, A.C., Finzi, A., Daly, E., Vargas, R.
876 and Novick, K.A.: Changes in photosynthesis and soil moisture drive the seasonal soil
877 respiration-temperature hysteresis relationship. *Agric. For. Meteorol.*, 259:184-195, doi:
878 10.1016/j.agrformet.2018.05.005, 2018.

879 Zhang, Y. Q., Yu, Q., Jiang, J., and Tang, Y. H.: Calibration of Terra/MODIS gross primary
880 production over an irrigated cropland on the North China Plain and an alpine meadow on the
881 Tibetan Plateau, *Global Change Biol.*, 14, 757-767, doi: 10.1111/j.1365-2486.2008.01538.x,
882 2008.

883 Zhao, M. S., Heinsch, F. A., Nemani, R. R., and Running, S. W.: Improvements of the MODIS
884 terrestrial gross and net primary production global data set, *Remote Sens. Environ.*, 95,
885 164-176, doi: 10.1016/j.rse.2004.12.011, 2005.

Table 1 Carbon content of different parts (gC kg⁻¹ DM)

crop	date	root	stem	green leaf	dead leaf	grain
wheat	3/15/2011	416	413	488	-	-
	3/22/2011	454	-	476	-	-
	3/29/2011	-	436	451	-	-
	4/5/2011	527	431	534	-	-
	4/13/2011	348	417	457	-	-
	4/21/2011	434	415	522	-	-
	4/29/2011	410	443	510	-	-
	5/6/2011	434	423	481	-	-
	5/14/2011	275	445	485	-	-
	5/22/2011	380	474	-	538	470
	5/29/2011	461	515	503	444	479
	6/5/2011	393	432	439	400	432
6/10/2011	393	429	-	426	449	
maize	7/4/2011	339	351	476	-	-
	7/13/2011	370	392	455	-	-
	7/21/2011	389	418	463	-	-
	7/29/2011	406	432	462	-	-
	8/5/2011	399	429	481	-	-
	8/12/2011	443	439	469	-	-
	8/22/2011	403	462	469	-	-
	9/3/2011	386	466	499	-	446
	9/11/2011	466	465	505	-	460
	9/20/2011	445	481	481	-	454
	9/30/2011	439	481	489	457	462

Table 2 Various ratios associated with carbon fluxes in croplands

crop species	ER/GPP	R _A /GPP ^a	R _H /ER	R _{AB} /ER	R _{AA} /ER	source
maize	0.69	0.32	0.54	0.21	0.25	this study
maize	0.67	0.56	0.16	0.25	0.59	Jans et al. (2010)
maize	0.85	0.45	0.47	0.02	0.51	Wang et al. (2015)
maize	0.80	0.65	0.19	0.21	0.60	Demyan et al. (2016) ^b
wheat	0.59	0.24	0.59	0.21	0.20	this study
wheat	0.71	0.49	0.31	0.19	0.50	Demyan et al. (2016) ^b
wheat	0.61	0.46	0.24	0.31	0.45	Moureaux et al. (2008)
wheat (2005)	0.60	0.44	0.26		0.74	Aubinet et al. (2009) ^c
wheat (2007)	0.57	0.48	0.15		0.85	Aubinet et al. (2009) ^c
wheat	0.57	0.45	0.21	0.17	0.62	Suleau et al. (2011)
wheat	0.66	0.43	0.35	0.05	0.59	Wang et al. (2015)
potato	0.48	0.37	0.24		0.76	Aubinet et al. (2009) ^c
potato	0.47	0.32	0.33	0.14	0.53	Suleau et al. (2011)
sugar beet	0.44	0.30	0.31		0.69	Aubinet et al. (2009) ^c
sugar beet	0.36	0.22	0.37	0.25	0.36	Suleau et al. (2011)

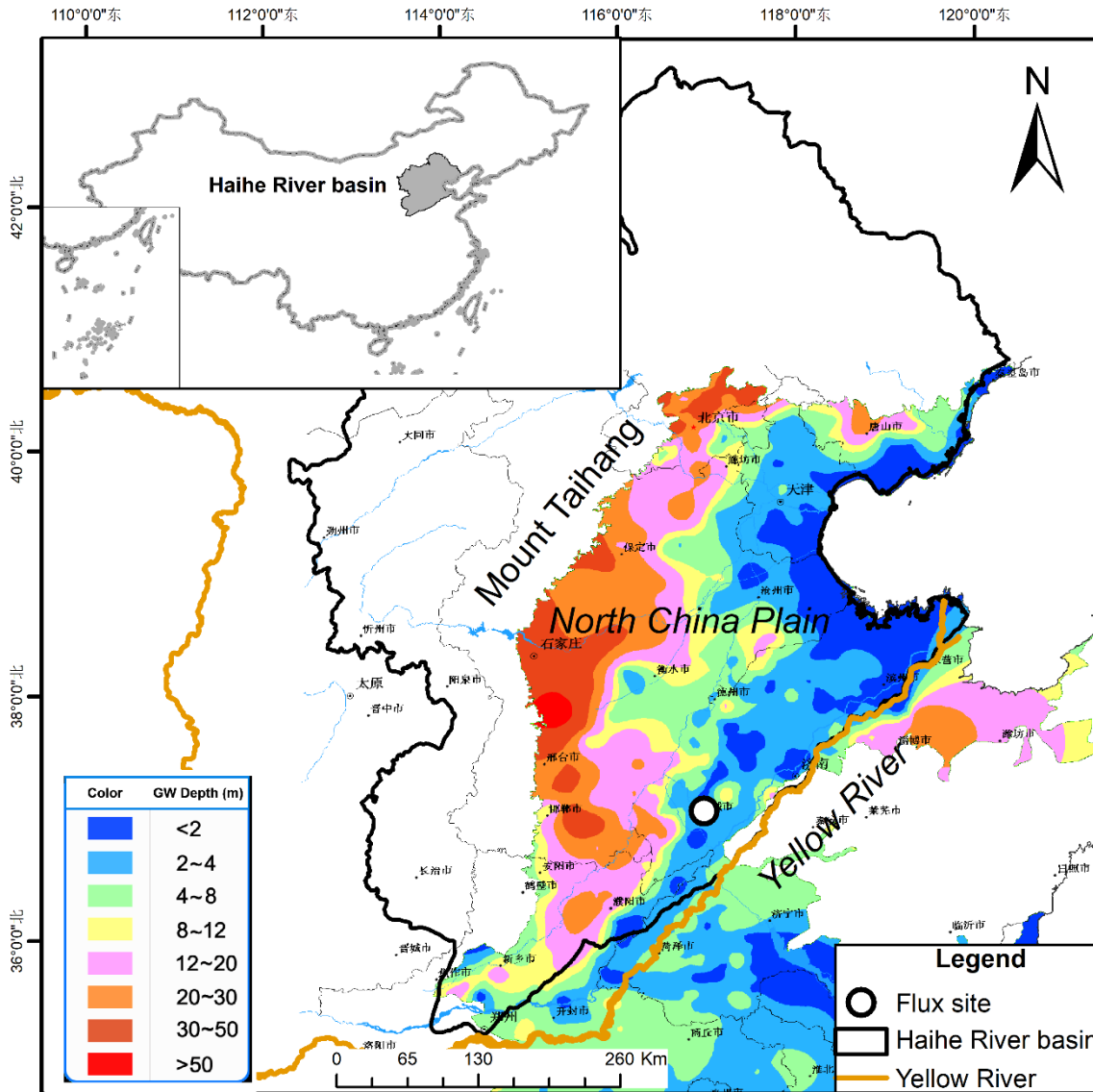
890 Note:

891 a- the values in parentheses indicate that the value is calculated by the equation $R_A/GPP=1-NPP/GPP$.

892 b- The data was from 2012, and the estimation is based on the average of the static and dynamic methods

893 c- R_A as well as R_H is the averaged values of their two corresponding methods

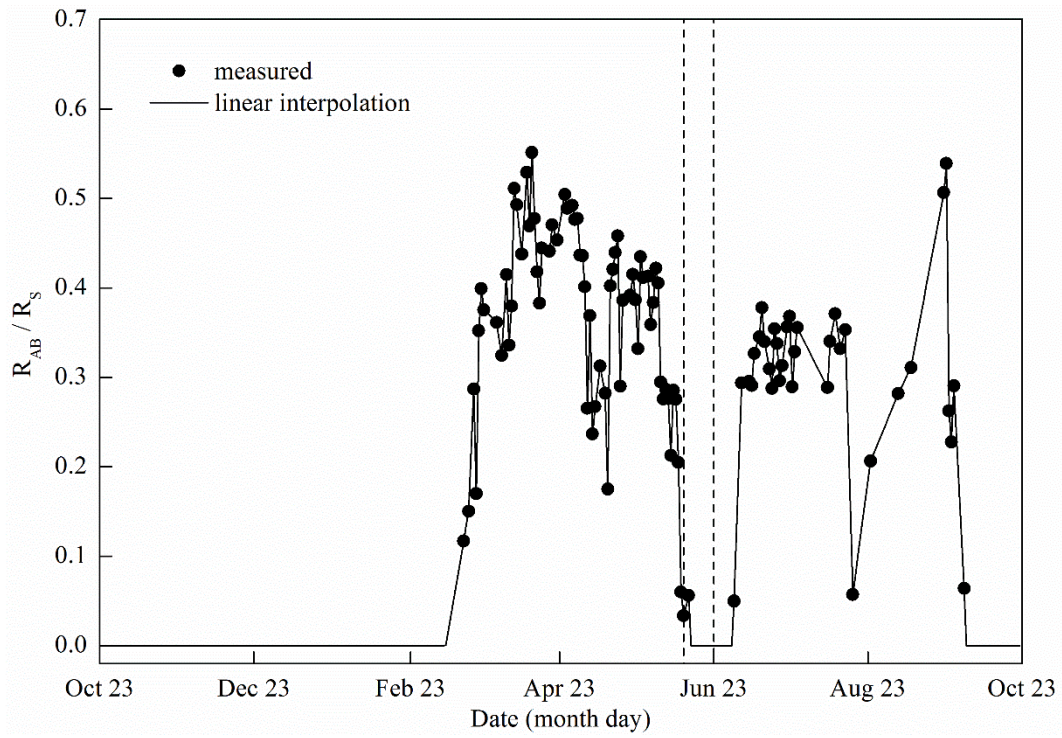
894



895

896 Fig. 1 Location of the experimental site. The background is the shallow groundwater depth in

897 early September of 2011 (modified from <http://dxs.hydroinfo.gov.cn/shuiziyuan/>)

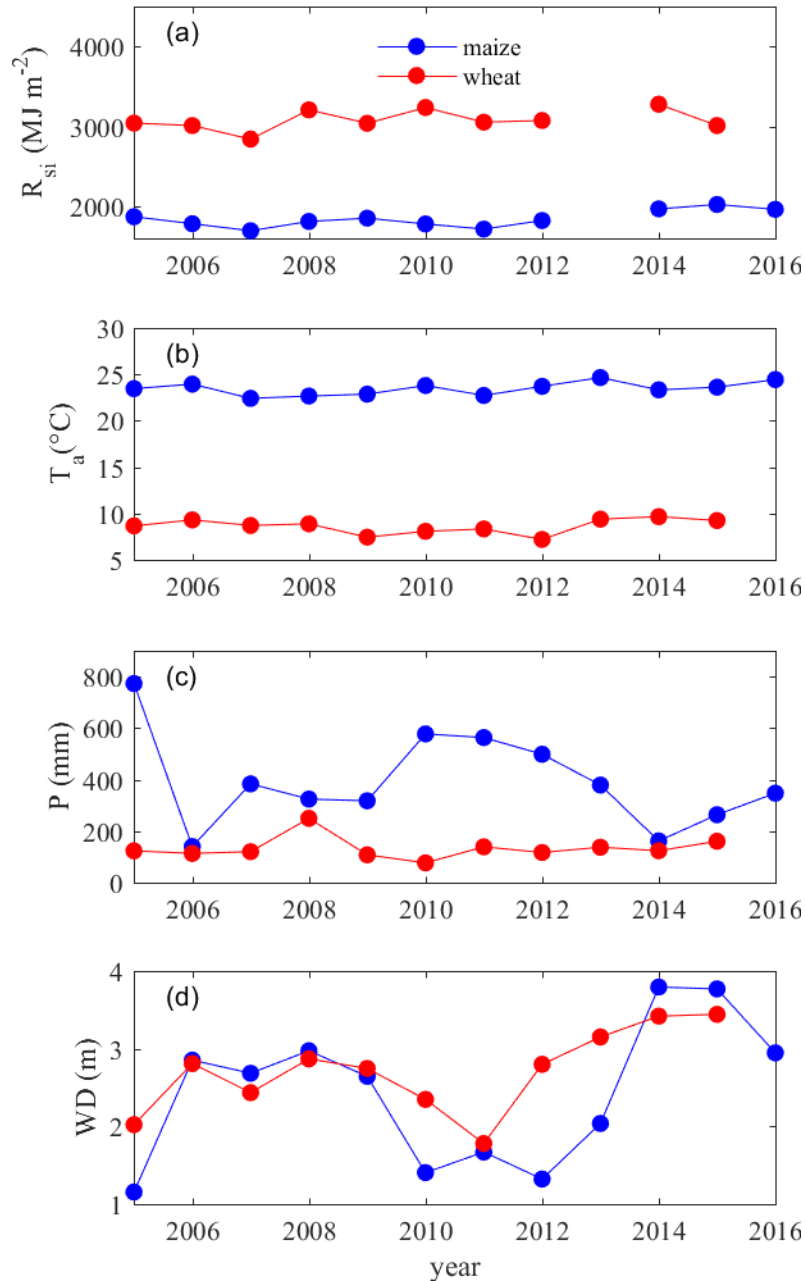


898

899 Fig. 2 Seasonal variations in the ratio of below-ground autotrophic respiration (R_{AB}) to total

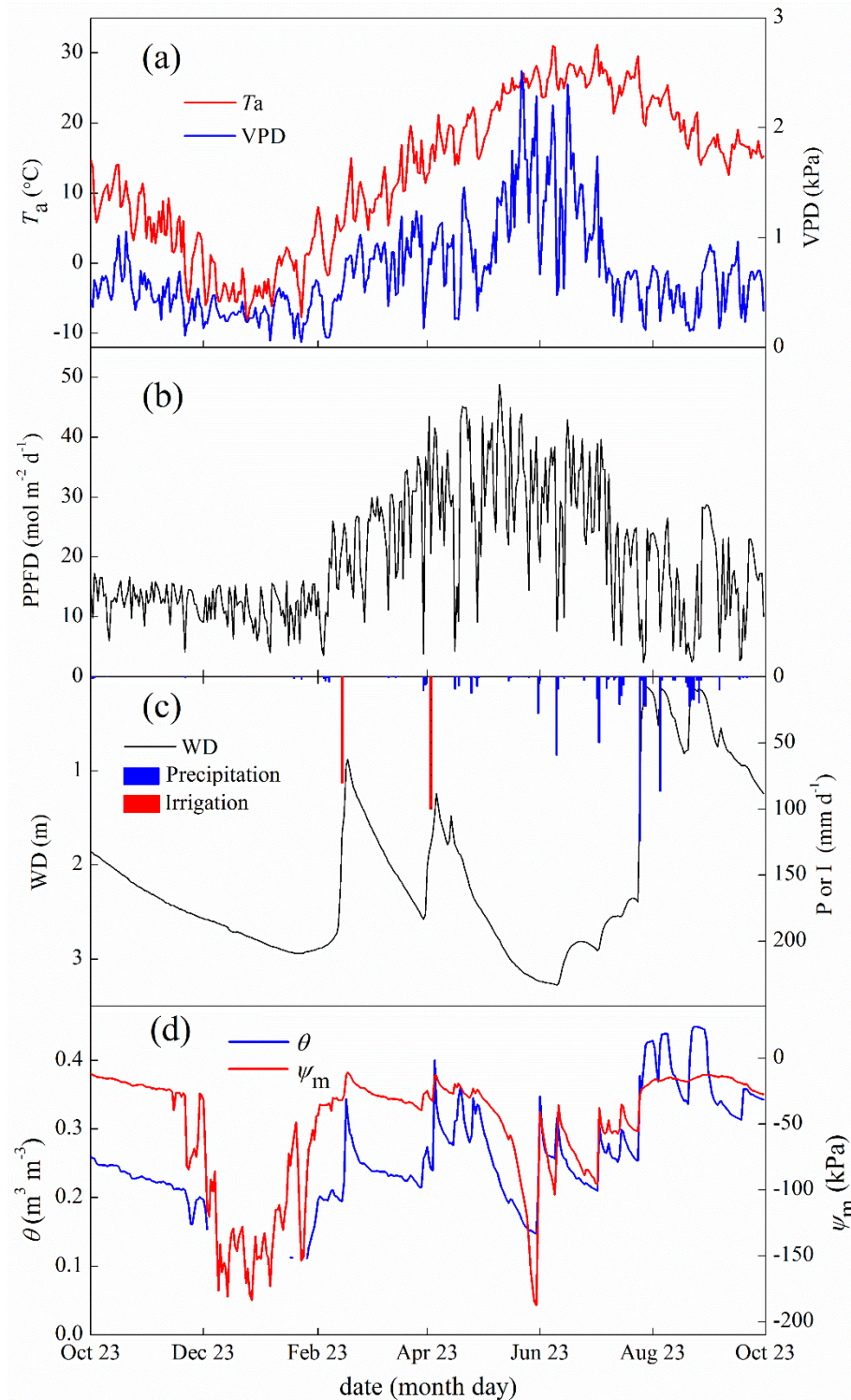
900 soil respiration (R_S). Two vertical dashed lines (hereafter) represent the date of harvesting

901 wheat and sowing maize, respectively.



902
 903
 904
 905
 906

Fig. 3 The seasonal (a) total incoming short-wave radiation (R_{si}), (b) average air temperature (T_a), (c) total precipitation (P) and (d) average groundwater depth (D) for both wheat and maize evaluated for the period from 2005 through 2016. Note that incoming short-wave radiation in the 2013 season was missing due to equipment malfunction.



907

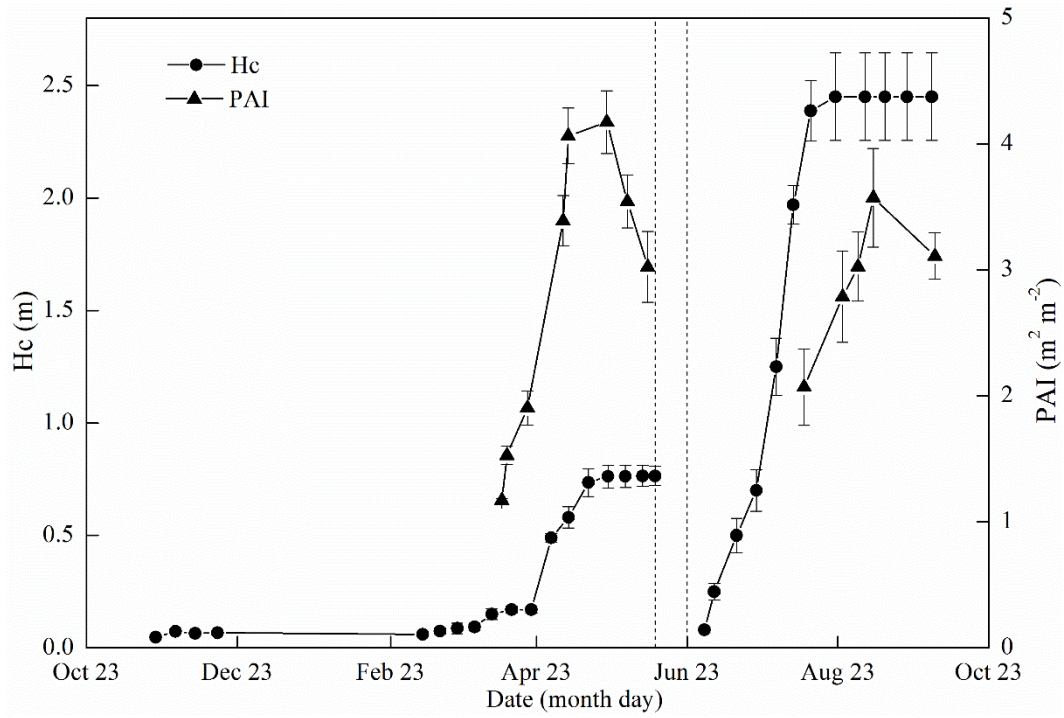
908

909

910

911

Fig. 4 Seasonal variations in the environmental variables of (a) air temperature (T_a), soil temperature at 5cm depth (T_s) and vapor pressure deficit (VPD), (b) photosynthetic photon flux density (PPFD), (c) precipitation (P), irrigation (I) and groundwater depth (WD), and (d) volumetric soil moisture (θ) and soil matric potential (ψ_m).

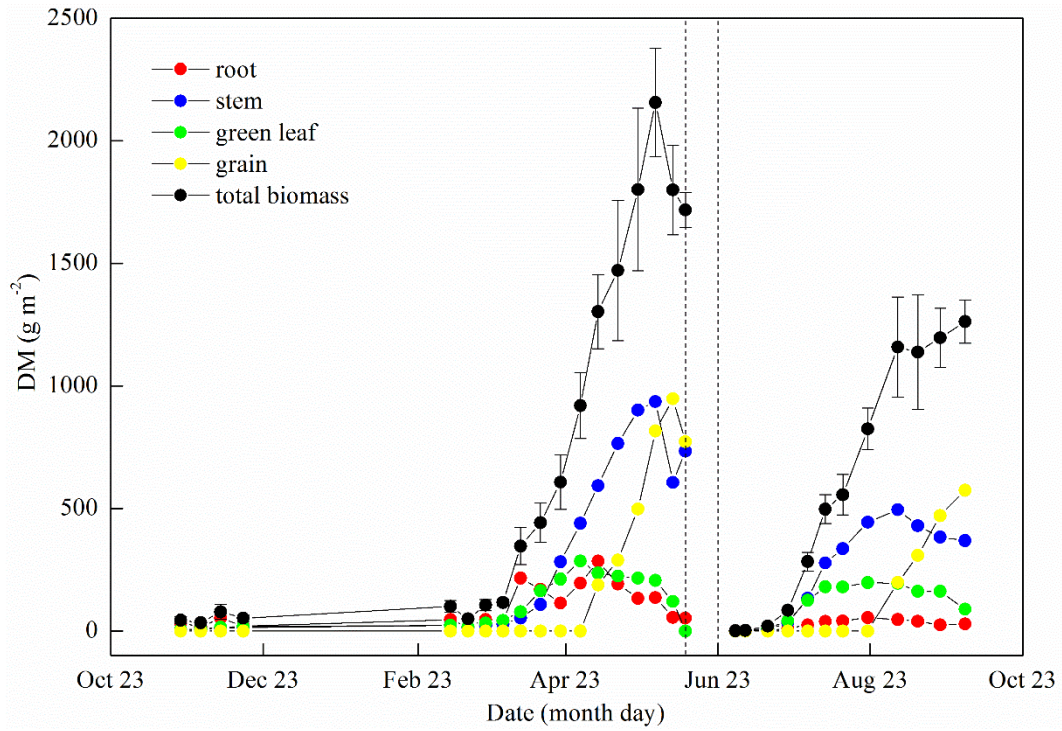


912

913 Fig. 5 Seasonal variations in canopy height (H_C) and plant area index (PAI). The error bars

914

denote 1 standard deviation of the ten points.



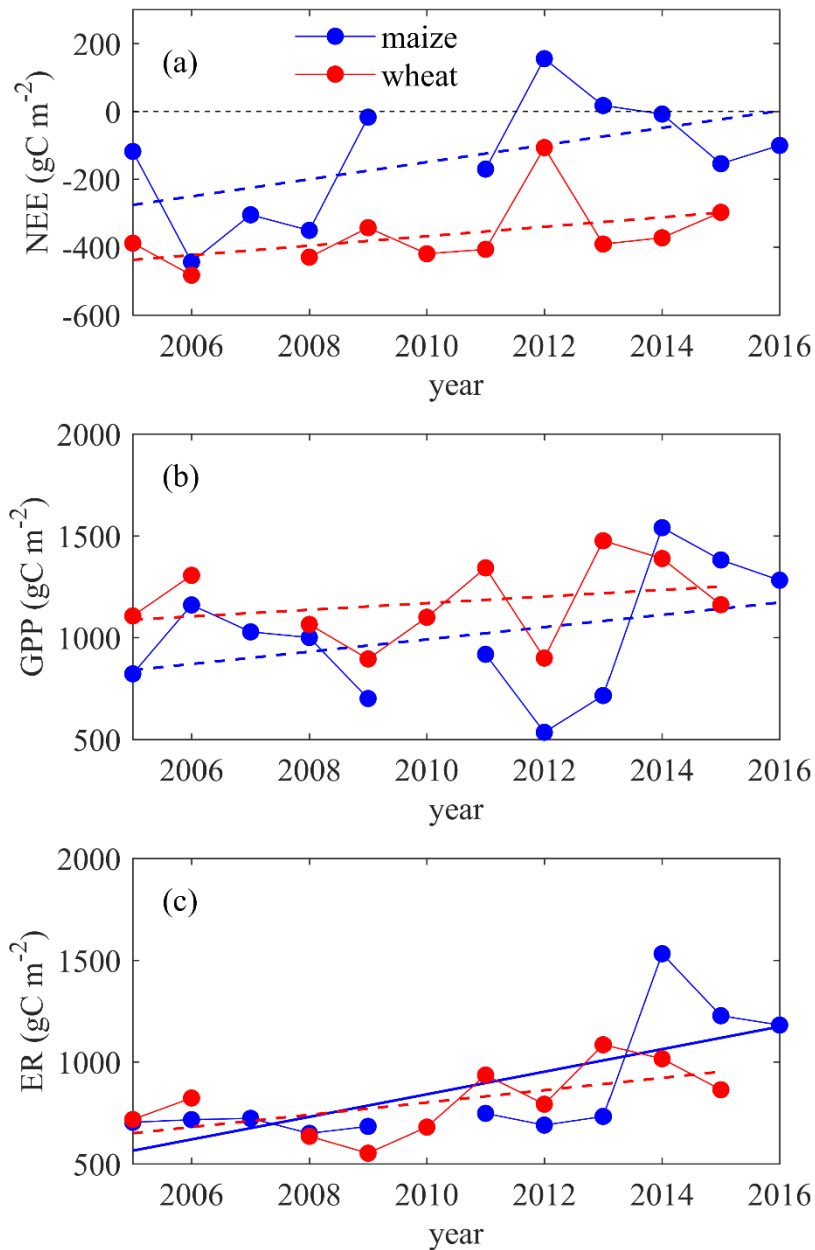
915

916

Fig. 6 Seasonal variations in the total dry biomass (DM) and its major parts of root, stem,
 917 green leaf and grain. The error bars of total biomass denote 1 standard deviation of the four

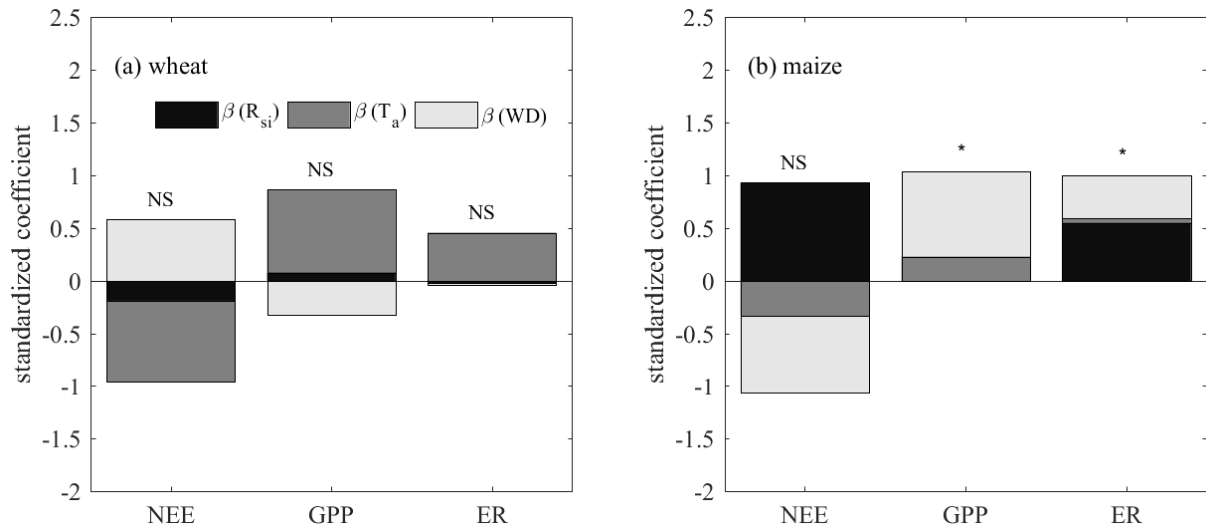
918

sample points.



919

920 Fig. 7 The temporal trend of annual (a) Net Ecosystem Exchange (NEE), (b) Gross Primary
 921 Productivity (GPP) and (c) Ecosystem Respiration (ER) for both wheat and maize from 2005
 922 through 2016. Note that though most gaps of carbon fluxes were filled, the wheat of 2007 was
 923 excluded as it had a large gap accounting for 26 % of annual records unable to fill; maize was
 924 not planted in the growing season of 2010. Note that the solid line represents the temporal
 925 trend passes F-test at $p < 0.05$ significance level, while the dashed line represents the temporal
 926 trend does not pass the F-test at $p < 0.05$ level.



927

928

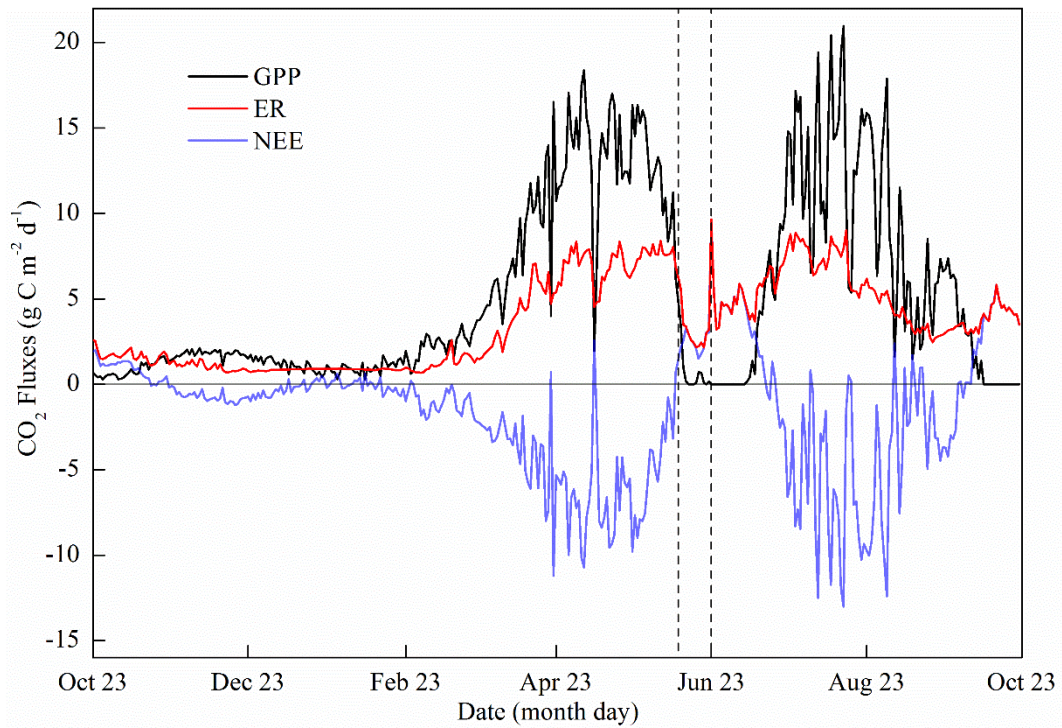
929

930

931

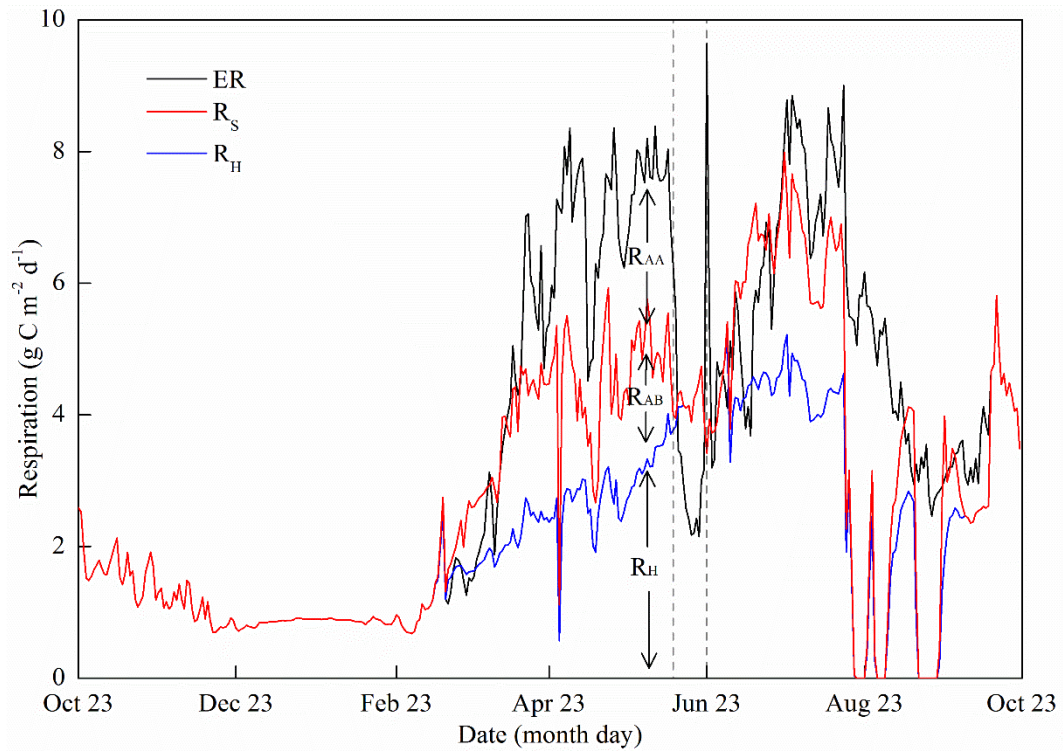
Fig. 8 The result of multiple regression for NEE, GPP and ER with incoming short-wave radiation (R_{si}), air temperature (T_a) and [groundwater depth](#) (WD) for both (a) wheat and (b) maize. Note that * denotes that the regression passes $p < 0.05$ significance level, and NS indicates non-significant.

932



933

934 Fig. 9 Seasonal variations in Gross Primary Productivity (GPP), Net Ecosystem Exchange
935 (NEE) and Ecosystem Respiration (ER) (those before April 2nd were calculated with SVR
936 method)



937

938

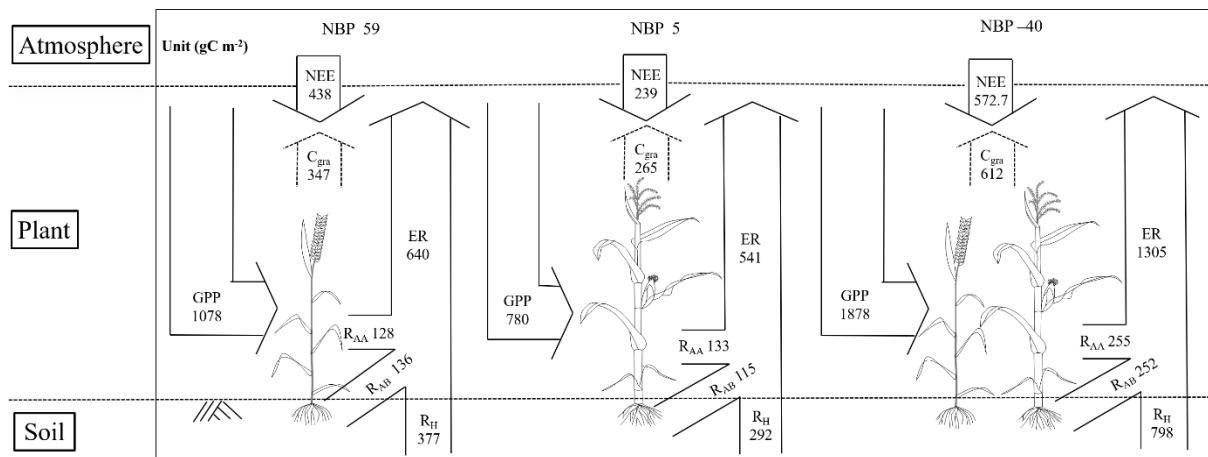
939

940

941

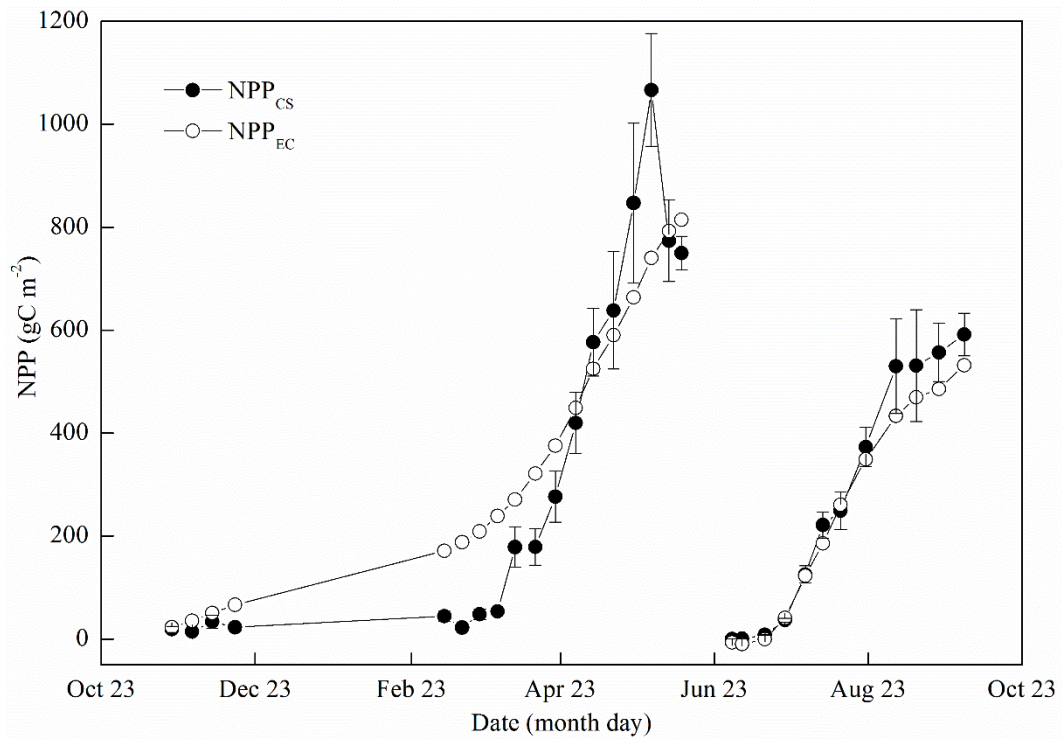
942

Fig. 10 Seasonal variations in the components of Ecosystem Respiration (ER), total soil respiration (R_S), soil heterotrophic respiration (R_H). The difference between ER and R_S denotes above-ground autotrophic respiration (R_{AA}), and the difference between R_S and R_H denotes below-ground autotrophic respiration (R_{AB}).



943
 944
 945
 946
 947

Fig. 11 Carbon budget of wheat (left), maize (middle) and the full wheat-maize rotation cycle with fallow periods included (right). Note that absolute value of NEE is shown here; NBPs of wheat and maize are the average of two independent methods (i.e, eddy covariance-based and crop sample-based)



948

949

950

951

Fig. 12 Seasonal variations in the cumulative Net Primary Productivity (NPP) with two independent methods of Crop Sample (NPP_{CS}) and Eddy Covariance (NPP_{EC}) complemented with soil respiration measurements.